Development of high vorticity structures in incompressible 3D Euler equations.

D. Agafontsev [(a)], A. Mailybaev [(b), (c)] and E. Kuznetsov [(d)].

[(a)] - P.P. Shirshov Institute of Oceanology of RAS, Moscow, Russia.

[(b)] - Instituto Nacional de Matematica Pura e Aplicada - IMPA, Rio de Janeiro, Brazil.

[(c)] - Institute of Mechanics, Lomonosov Moscow State University, Russia.

[(d)] - P.N. Lebedev Physical Institute of RAS, Moscow, Russia.

Solitons, Collapses and Turbulence – 2014.
August 4-8, 2014, Chernogolovka, Russia.

1. Introduction.

The question of whether the incompressible Euler equations in three dimensions,

$$\frac{\partial \mathbf{v}}{\partial t} + (\mathbf{v}\cdot\nabla)\mathbf{v} = -\nabla p, \qquad \mathrm{div}\,\mathbf{v} = 0,$$

can develop a finite time singularity, or blow-up, from smooth initial velocity distribution with finite energy is the long-standing open problem in fluid dynamics.

This question is of fundamental importance, as the blow-up may be related to the onset of turbulence and to how the process of the energy transfer from large scales to small scales is arranged. Collapses usually drastically amplify the energy transfer to small scales, where in turn it is effectively dumped by viscosity.

It is known how the singularities should look like for 3D Euler equations: the small-scale structures of high vorticity,

$$\omega = \mathrm{rot}\ \mathbf{v},$$

with vorticity decaying quickly in one spacial direction, and very slowly in two other directions; the vorticity in this regions goes to infinity with time.

1. Introduction.

Kolmogorov spectra of turbulence: in case of the developed hydrodynamic turbulence with large Reynolds numbers Re >> 1, the energy spectrum

$$\varepsilon(k,t) = \int |\mathbf{v}(\mathbf{k})|^2 k^2 do, \quad E = \int \varepsilon(k,t)\, dk = const,$$

in the inertial interval is determined by the constant energy transfer P through the scales (dimensional analysis):

$$\varepsilon(k,t) = const \times P^{2/3} \times k^{-5/3}.$$

The same dimensional analysis yields the following distribution for velocity fluctuation on the given scale ***r*** :

$$\mathrm{v} = const \times P^{1/3} \times r^{2/3}.$$

Then, for vorticity we have singular distribution:

$$\omega = const \times P^{1/3} \times r^{-1/3}.$$

These results are for the inertial interval, where the scales do not feel the pumping at large scales, and the dumping due to viscosity at small scales. Therefore, at the scale from the inertial interval we have 3D Euler equations. This means that Kolmogorov distributions should be applicable to 3D Euler equations as well.

Then, what are the physical mechanisms that shape such singular distribution of vorticity for 3D Euler equations? What are the mechanisms that ensure the constant energy transfer from large scales toward small scales?

1. Introduction.

One of the possible answers is that this vorticity distribution is singular because of the existence of real singularities in the vorticity field, and that these singularities at the same time are the sink that absorb the energy from large scales and ensure the creation of Kolmogorov spectra of turbulence.

Today there are two main hypothesis to how the singularities evolve with time: (1) exponential,

$$\max|\omega| \sim \exp(\alpha t),$$

and (2) blow-up,

$$\max|\omega| \sim (t_0 - t)^{-1}.$$

Both hypothesis ensure arrival to viscous scales in a finite time.

1. Introduction.

M.E. Brachet, M. Meneguzzi, A. Vincent, H. Politano, and P.L. Sulem. *Numerical evidence of smooth self-similar dynamics and possibility of subsequent collapse for three-dimensional ideal flows*. Physics of Fluids A: Fluid Dynamics (1989-1993), 4(12):2845-2854, 1992.

The first authors who demonstrated exponential development of singularities for vorticity field from smooth initial data. General periodic flows were studied on $\mathbf{256^3}$ grid, symmetric Taylor-Green vortex,

$$\mathrm{v}_x(t=0) = \sin(x)\cos(y)\cos(z),$$

$$\mathrm{v}_y(t=0) = -\cos(x)\sin(y)\cos(z),$$

$$\mathrm{v}_z(t=0) = 0,$$

- on $\mathbf{864^3}$ grid. The energy spectrum **ε(k)**, was shown to be well-approximated by the ansatz

$$\varepsilon(k,t) = ck^{n(t)}e^{-2\delta(t)k}.$$

The exponent **δ(t)** clearly behaved exponentially, the vorticity maximum also increased exponentially. Also, the authors found that the singularities represent a pancake structures, where vorticity quickly decays in one direction, and slowly – in two other directions.

1. Introduction.

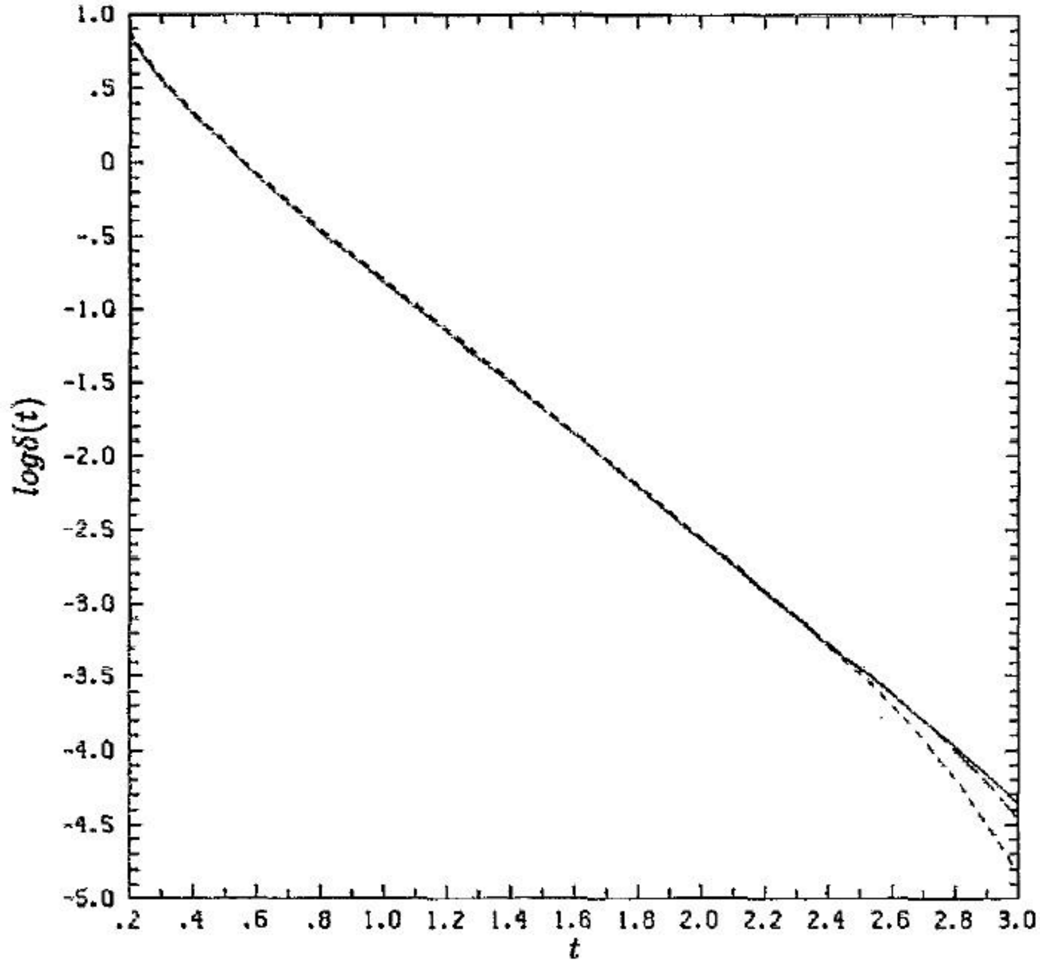

FIG. 2. Time evolution of the logarithmic decrement $\delta(t)$ obtained by fitting the energy spectrum on the ranges $5<k<71$, $5<k<161$, and $5<k<279$ for the inviscid Taylor–Green vortex integrated with resolutions 256^3 (dotted line), 512^3 (dashed line), and 864^3 (solid line), respectively.

1. Introduction.

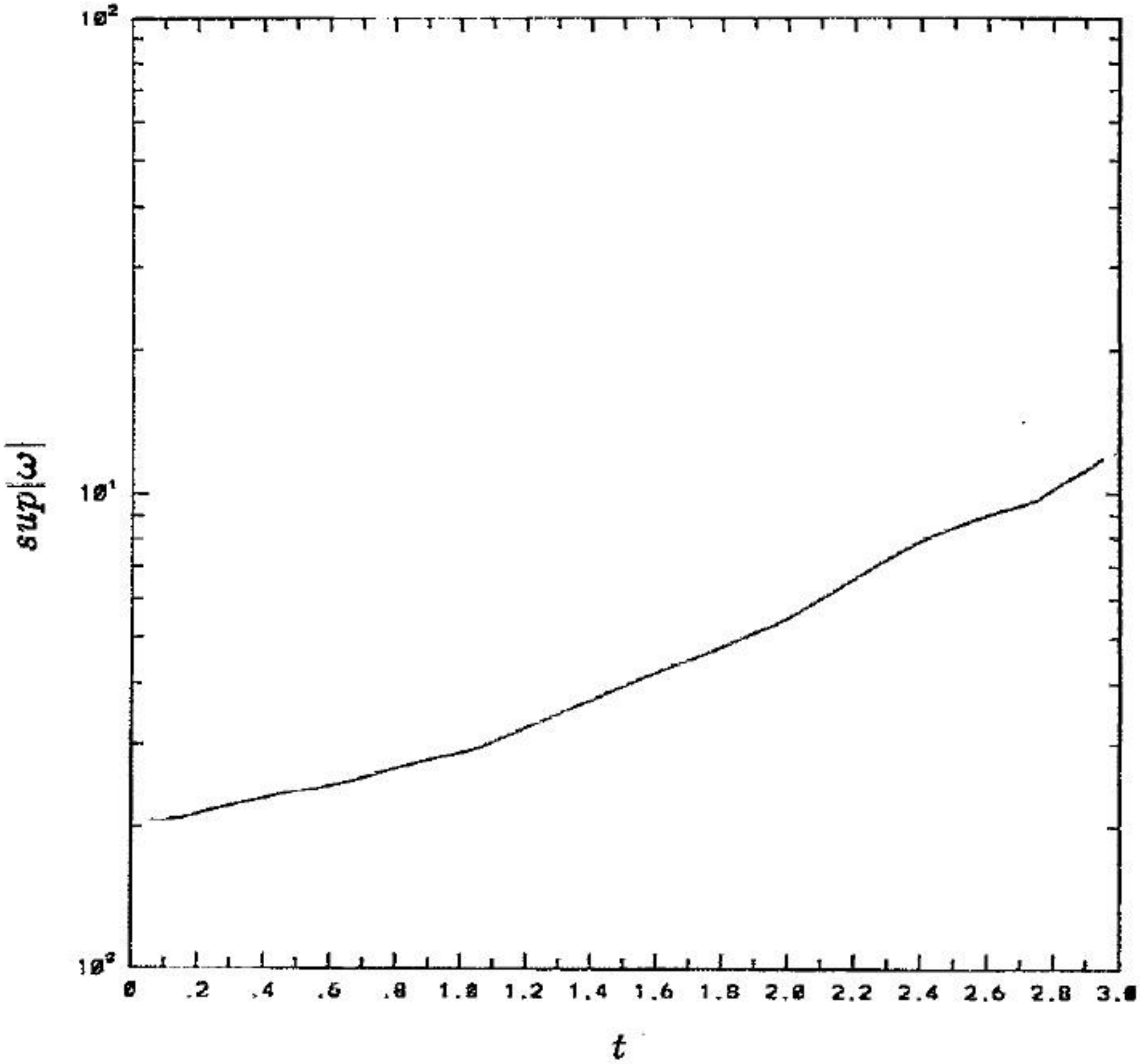

FIG. 6. Time evolution of the vorticity maximum sup$|\omega|$ for the random periodic flow at resolution 256^3.

1. Introduction.

In the next 20 years people mainly concentrated on the testing of specially designed initial data in the hope that these initial data would provide them the blow-up scenario. There were several publications where the authors claimed that they found such initial data, and there were subsequent publications where these simulations were repeated on larger grids and with more accurate methods, and in the end it turned out that there are no sufficient data to back-up the blow-up hypothesis.

It turned out also, that this is the normal situation when very large grids are necessary to achieve even sufficiently small vorticity maximum increase with time.

1. Introduction.

T. Grafke, H. Homann, J. Dreher, and R. Grauer. ***Numerical simulations of possible finite time singularities in the incompressible euler equations: comparison of numerical methods.*** **Physica D: Nonlinear Phenomena, 237(14):1932–1936, 2008.**

Different spectral and real-space methods, Pelz-Kida like initial flow: 2-fold maximum increase for $\mathbf{512^3}$ grid and 3-fold - for $\mathbf{1024^3}$ grid before the methods started to diverge.

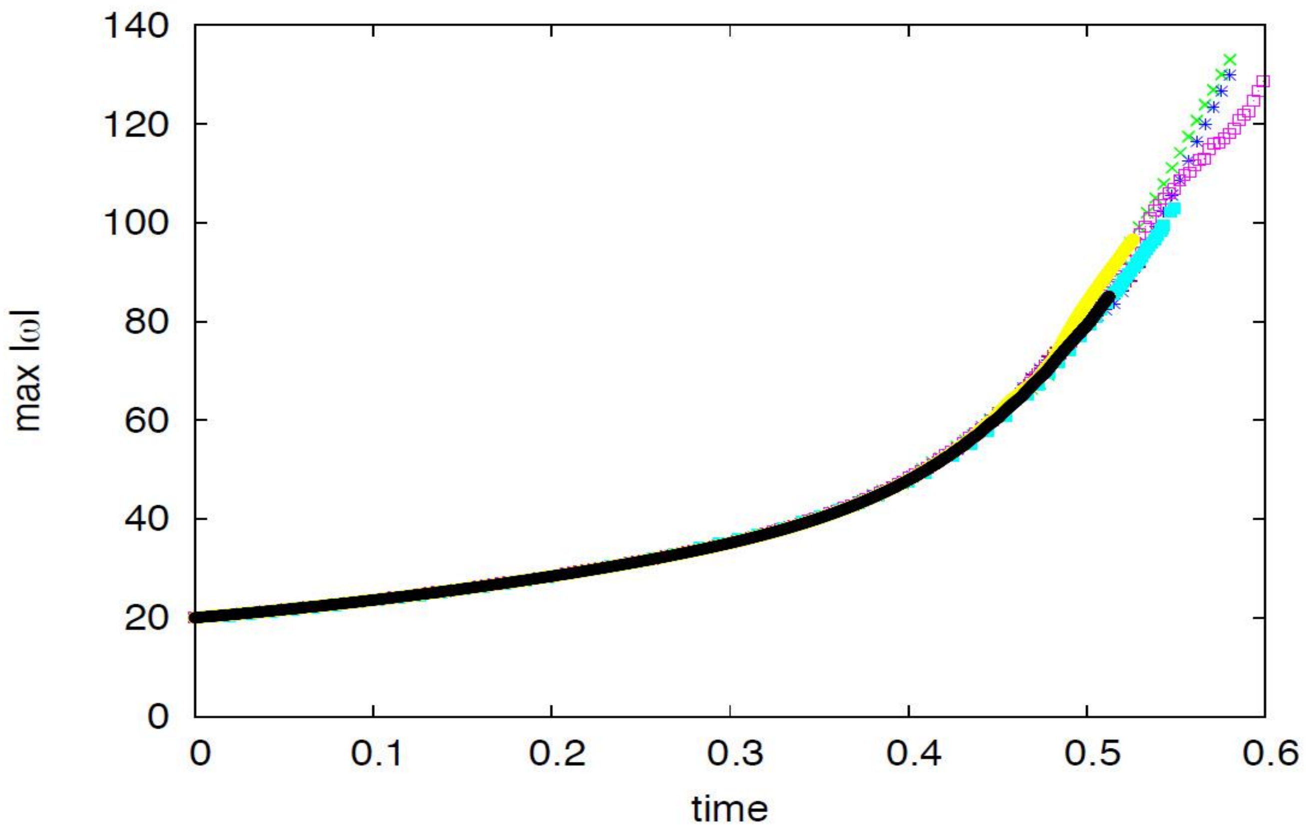

FIG. 1: Growth of max $|\boldsymbol{\omega}|$ for all implemented numerical schemes.

1. Introduction.

In our opinion, despite the large effort we are still far from the reliable answer of whether the blow-up scenario is possible. And from the point of view of numerical simulations, there is no much hope that we will achieve this answer anytime soon.

This is why we decided to move in a different direction in our study.

First, we do not concentrate on specially designed initial data, and test random periodic flows.

Second, we track down not only the global maximum, but also all the remaining local maximums as well. And we concentrate on testing the distributions of these local maximums.

In our results we have small intervals of Kolmogorov spectra; our results show tendency with time toward the Kolmogorov spectra.

2. Numerical method.

(1) Huge memory requirements. One scalar array on **1024^3** grid of type real with double precision takes **8 Gb** of RAM. Runge-Kutta 4^{th} order scheme for 3D Euler equations on the same grid requires about **130 Gb** of RAM. All this RAM must be places physically inside one motherboard, otherwise the interconnection between different machines dumps the speed by orders of magnitude. The corresponding figures for **2048^3** grid are **64 Gb** and **1100 Gb** respectively.

(2) Huge computational cost. Simulations on **1024^3** grid take months of work on modern CPUs. Usage of GPUs on large grids is not possible because of the required memory resources. In case of pseudo-spectral methods it is difficult to take advantage of parallelization because FFT does not parallelize very well in 3 dimensions.

(3) Dealiasing control: equations have quadratic nonlinearity, that gives us the standard 2/3-rule for dealiasing, that leaves us only **29%** of effective harmonics. Also, the bottle-neck instability, when the last 10% of harmonics rise too fast.

(4) Suppose we perform simulations on the best grid available. When we see that our spectrum starts to excite near the 2/3 aliasing point, we have to stop because of the aliasing error. But if we do so, we will get just 2-, 3-fold increase in global maximum.

This is why we have to continue, and perform the systematic convergence study of our results, comparing them with the results obtained using different grids.

2. Numerical method.

(5) The determination of local maximums in 3D is a very difficult problem. We work with very anisotropic distributions, when vorticity in the singularity regions decays quickly in one direction, and very slowly in two other directions.

The standard method, when we compare each points to its neighbors, doesn’t work: it gives about hundreds of local maximums per each pancake.

We had to develop a different method. The convergence study shows that we have errors in the number of local maximums within 10%.

2. Numerical method.

We solve 3D Euler equations in the periodic box **[-π, π]^3** in the vorticity formulation:

$$\frac{\partial \omega}{\partial t} = \mathrm{rot}\,(\mathbf{v} \times \omega), \quad \mathbf{v} = \mathrm{rot}^{-1}\omega,$$

that is obtained from the original 3D Euler equations by taking rotor operator of its both sides. This formulation is pressure-free. Inverse rotor operator is uniquely defined under the conditions of zeroth average velocity and incompressibility,

$$\int \mathbf{v} d^3\mathbf{r} = 0, \qquad \mathrm{div}\,\mathbf{v} = 0,$$

and has the simple representation in Fourier space as

$$\mathbf{v} = \frac{i\mathbf{k} \times \omega}{k^2}.$$

We implement Runge-Kutta 4th order scheme combined with the cut-off function for harmonics with high wavenumbers suggested by Hou & Li (2007),

$$\rho(\mathbf{k}) = \exp\left(-36\left[\left(k_1 / K_1\right)^{36} + \left(k_2 / K_2\right)^{36} + \left(k_3 / K_3\right)^{36}\right]\right).$$

2. Numerical method.

We start our simulations on **128³** grid. At every time step we analyze the spectrum of our solution, and if we determine that the spectrum starts to excite near

$$|k_i| \leq (2/3)K_i,$$

we immediately increase the number of points in this particular direction. Therefore, we choose number of points per each direction individually.

The distance between the subsequent harmonics is

$$\Delta k = 2\pi / L = 1,$$

and the range of the spectrum is

$$k_i \in [-\pi/\Delta x_i, +\pi/\Delta x_i] = [-N_i/2, +N_i/2].$$

We transfer the spectrum of our solution to the new grid, and set all the newly added harmonics to zero. The errors of such interpolation are comparable with the round-off errors.

When the grid approaches to the maximum grid allowed (fixed by RAM resources), we fix it, and continue our simulations beyond the 2/3-rule until the harmonics with large wavenumbers reach

$$|\omega_{2K/3}|^2 \leq 10^{-13} \max |\omega_k|^2 .$$

In the end of our simulations we have grids like **486 x 1024 x 2048**, or **1152 x 384 x 2304**.

3. Simulation results.

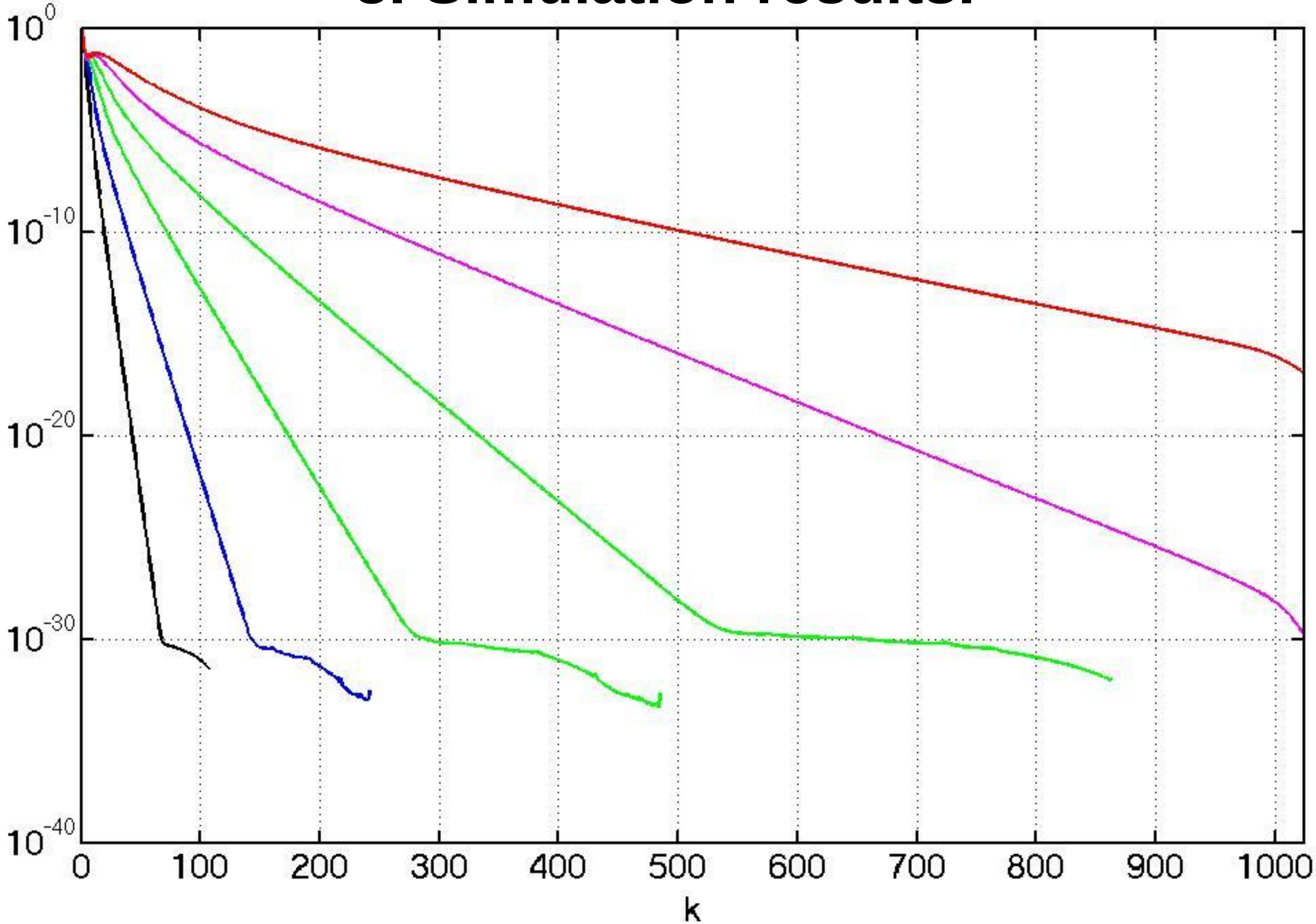

Evolution of the averaged over angles spectrum of vorticity field:

$$w(k,t) = \int |\omega(\mathbf{k})|^2 k^2 do,$$

t = 1.89 (black), t = 2.89 (blue), t = 3.89 (cyan), t = 4.89 (green), t = 5.89 (pink), t = 6.89 (red).

3. Simulation results.

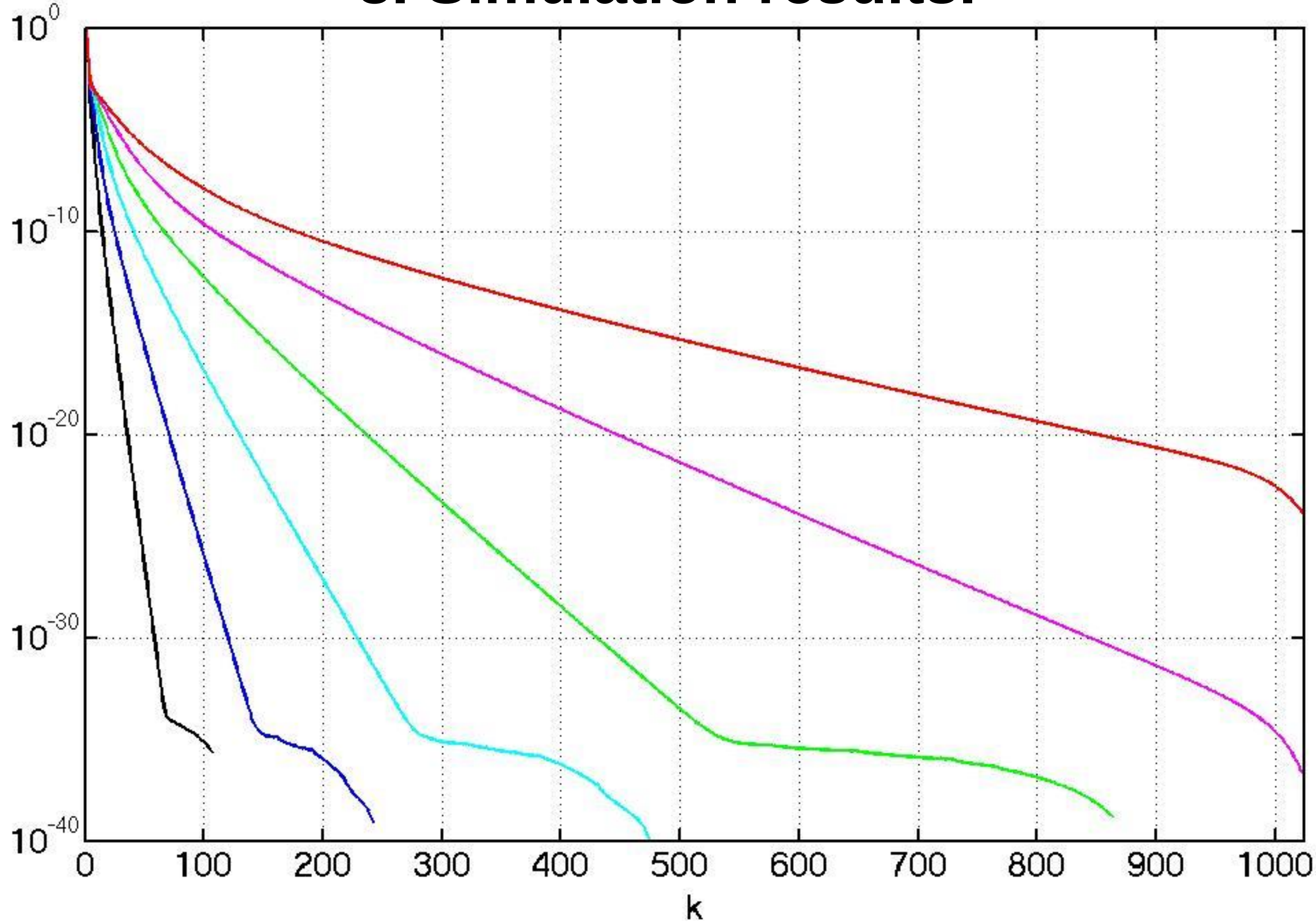

Evolution of the averaged over angles energy spectrum:

$$\varepsilon(k,t) = \int |\mathbf{v}(\mathbf{k})|^2 k^2 do, \quad |\mathbf{v}(\mathbf{k})|^2 = \frac{|\omega(\mathbf{k})|^2}{|\mathbf{k}|^2},$$

t = 1.89 (black), t = 2.89 (blue), t = 3.89 (cyan), t = 4.89 (green), t = 5.89 (pink), t = 6.89 (red).

3. Simulation results.

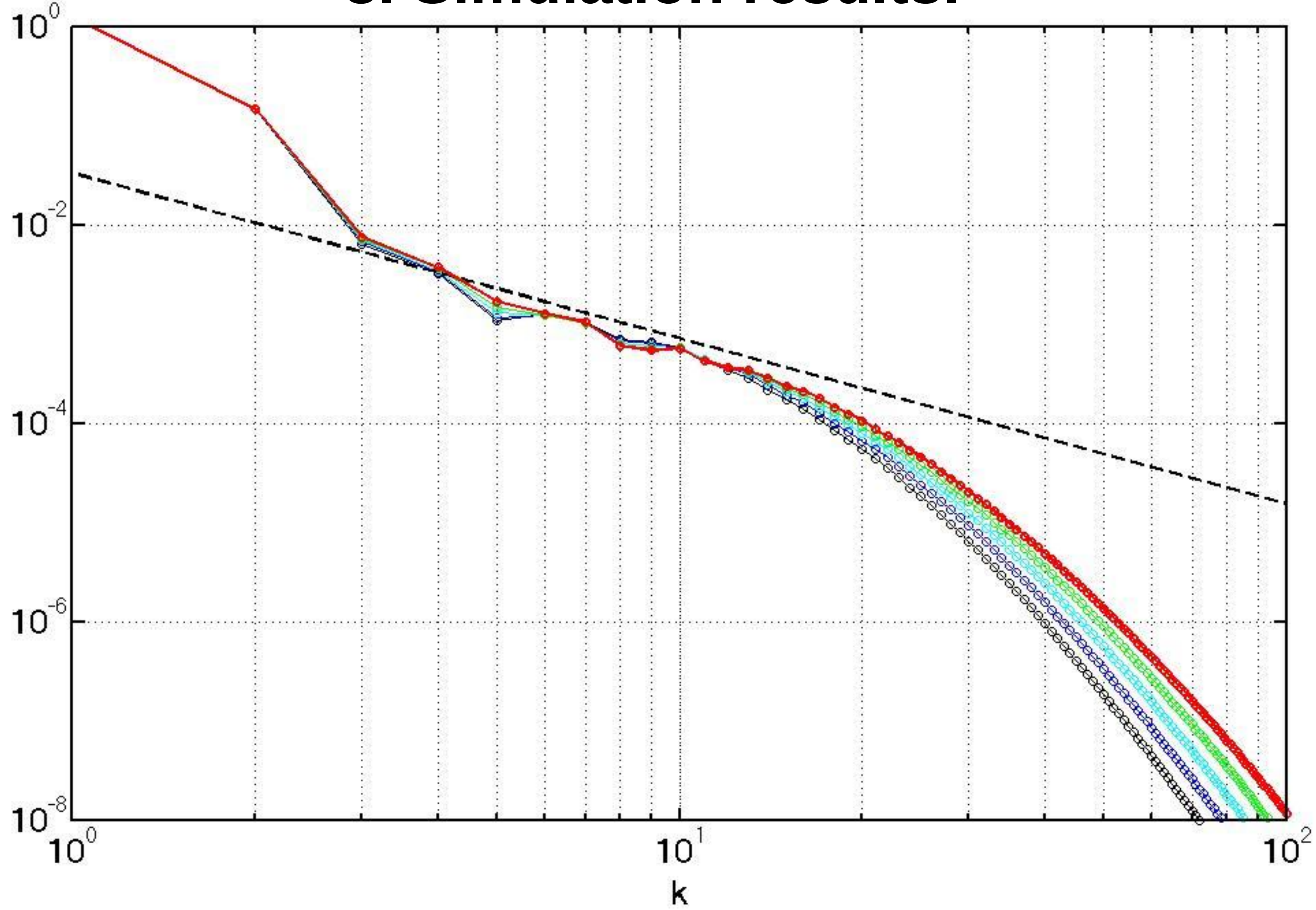

Tendency of the energy spectrum toward the Kolmogorov spectrum: for some of the wavenumbers, **3 ≤ k ≤ 16**, we observe

$$\varepsilon(k,t) \to const \times k^{-5/3}.$$

t = 6.09 (black), t = 6.29 (blue), t = 6.49 (cyan), t = 6.69 (green), t = 6.89 (red).

3. Simulation results.

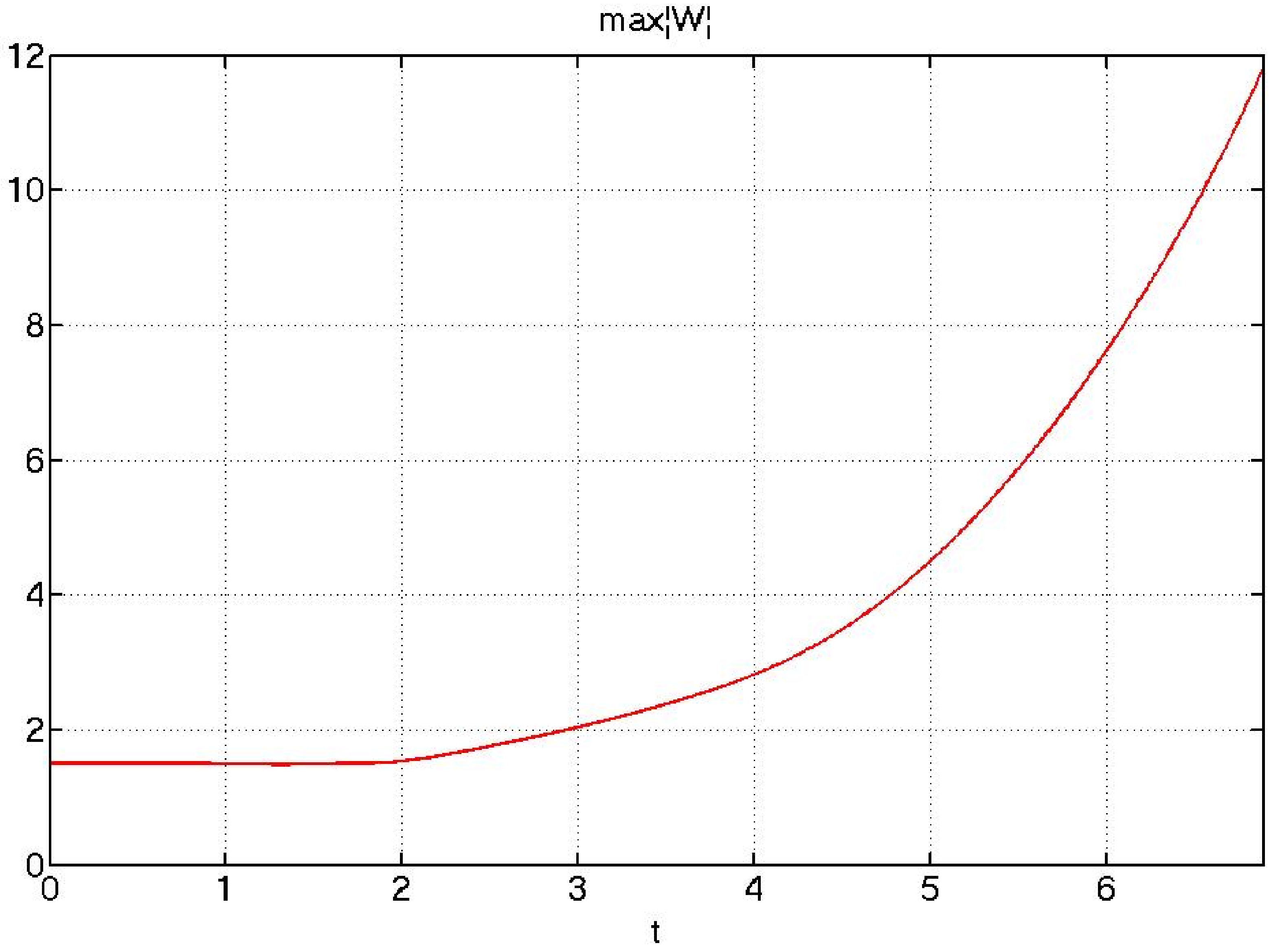

Evolution of vorticity maximum (global).

3. Simulation results.

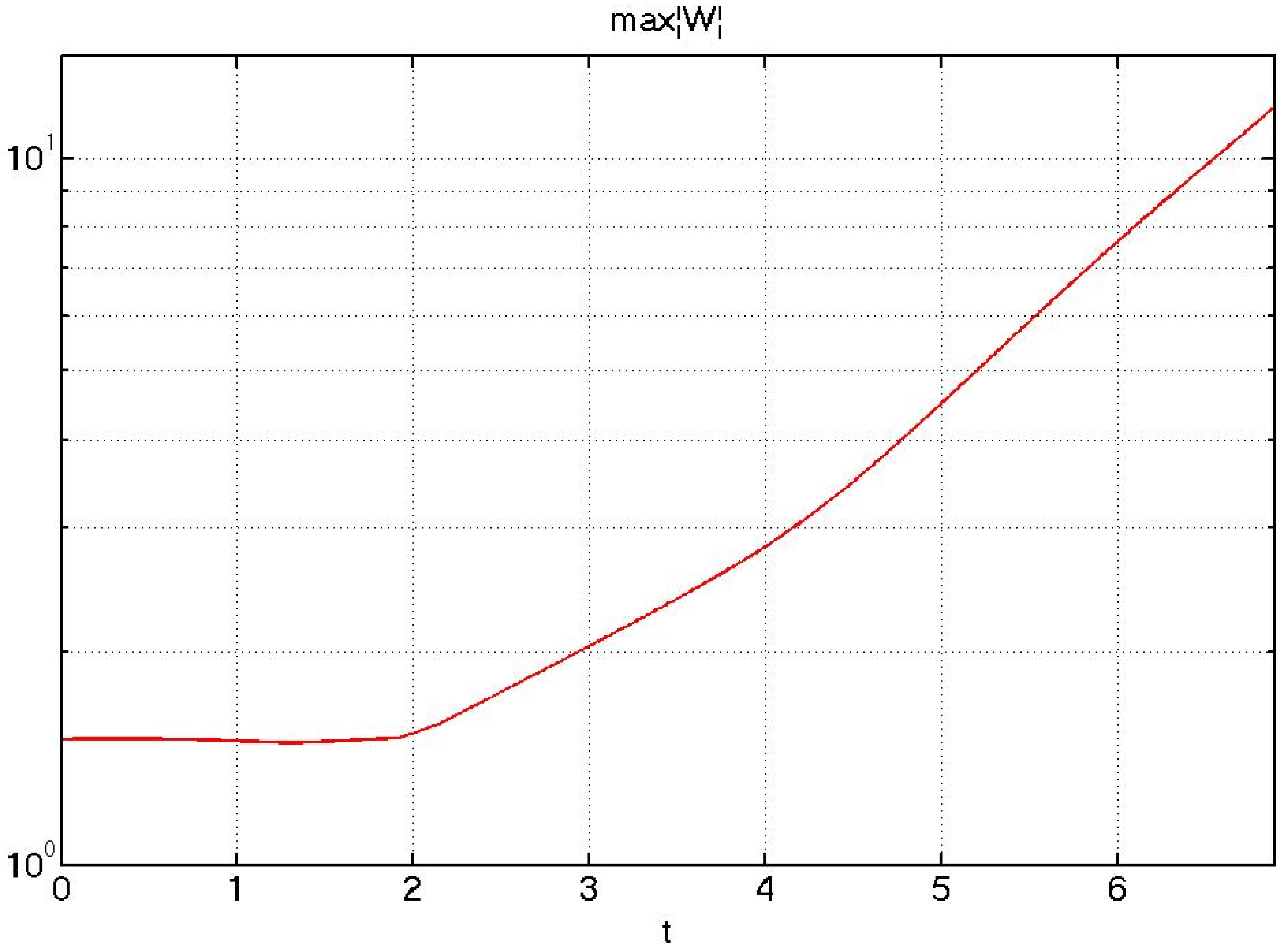

Evolution of vorticity maximum (global).

3. Simulation results.

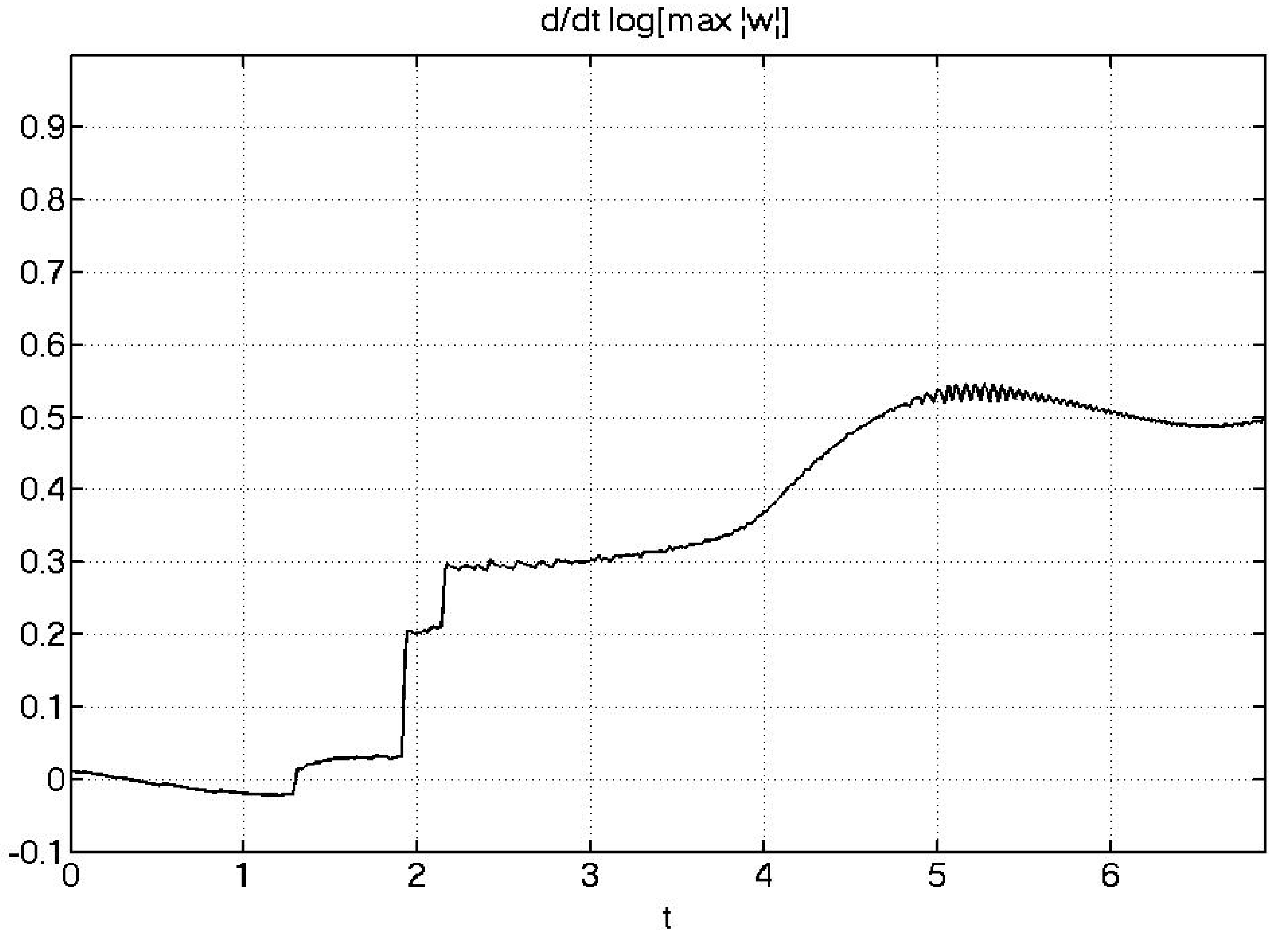

Exponential evolution: $\max|\omega| \sim exp(\alpha t), \quad \rightarrow \quad \frac{d}{dt}\log[\max|\omega|] \rightarrow const.$

Blow-up behavior: $\max|\omega| \sim \frac{1}{t_0 - t}, \quad \rightarrow \quad \frac{d}{dt}\log[\max|\omega|] \rightarrow \frac{1}{t_0 - t}.$

3. Simulation results.

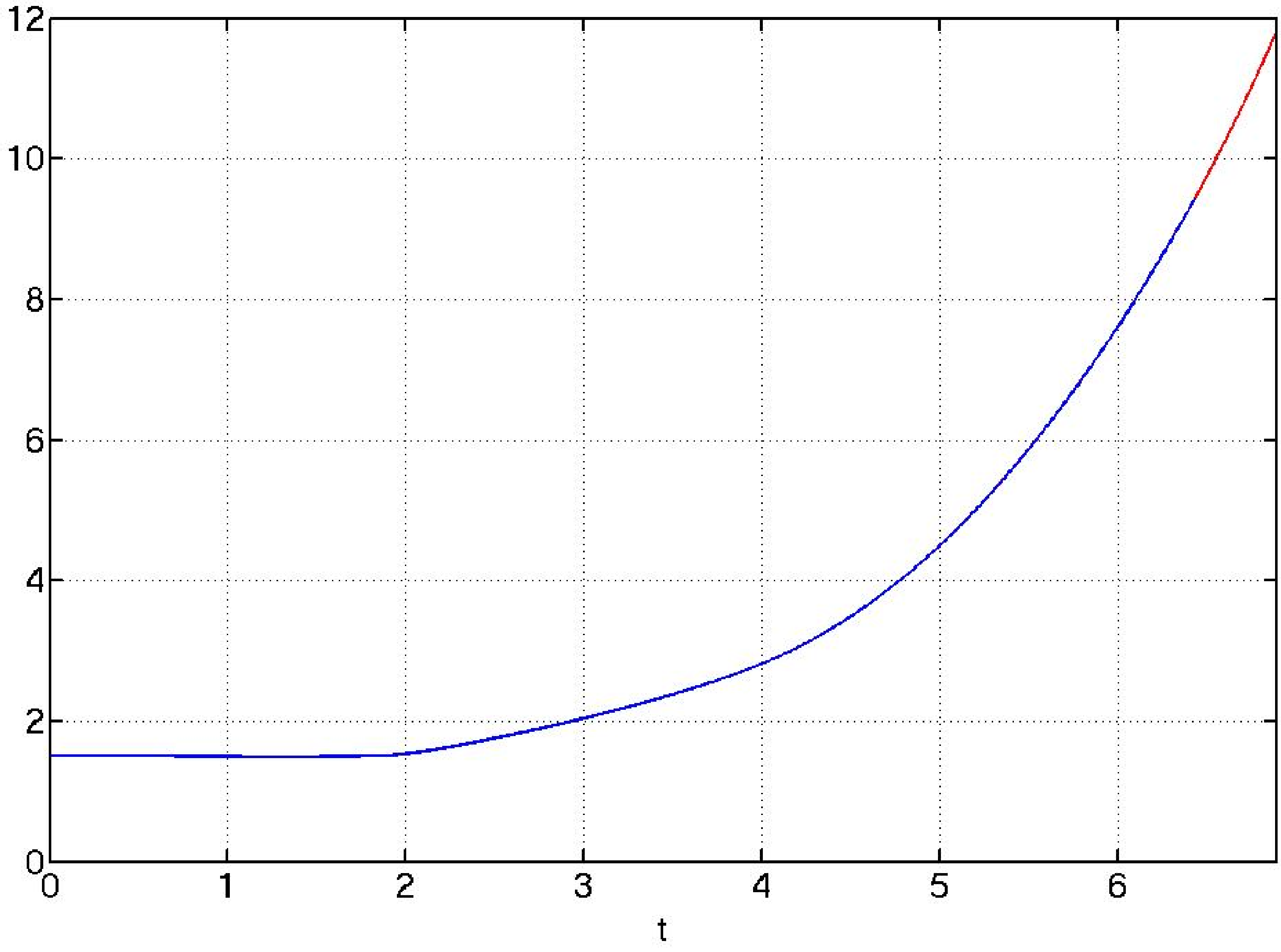

Evolution of vorticity maximum (global), convergence: blue – final grid **256 x 512 x 1024**; red – final grid **486 x 1024 x 2048**.

3. Simulation results.

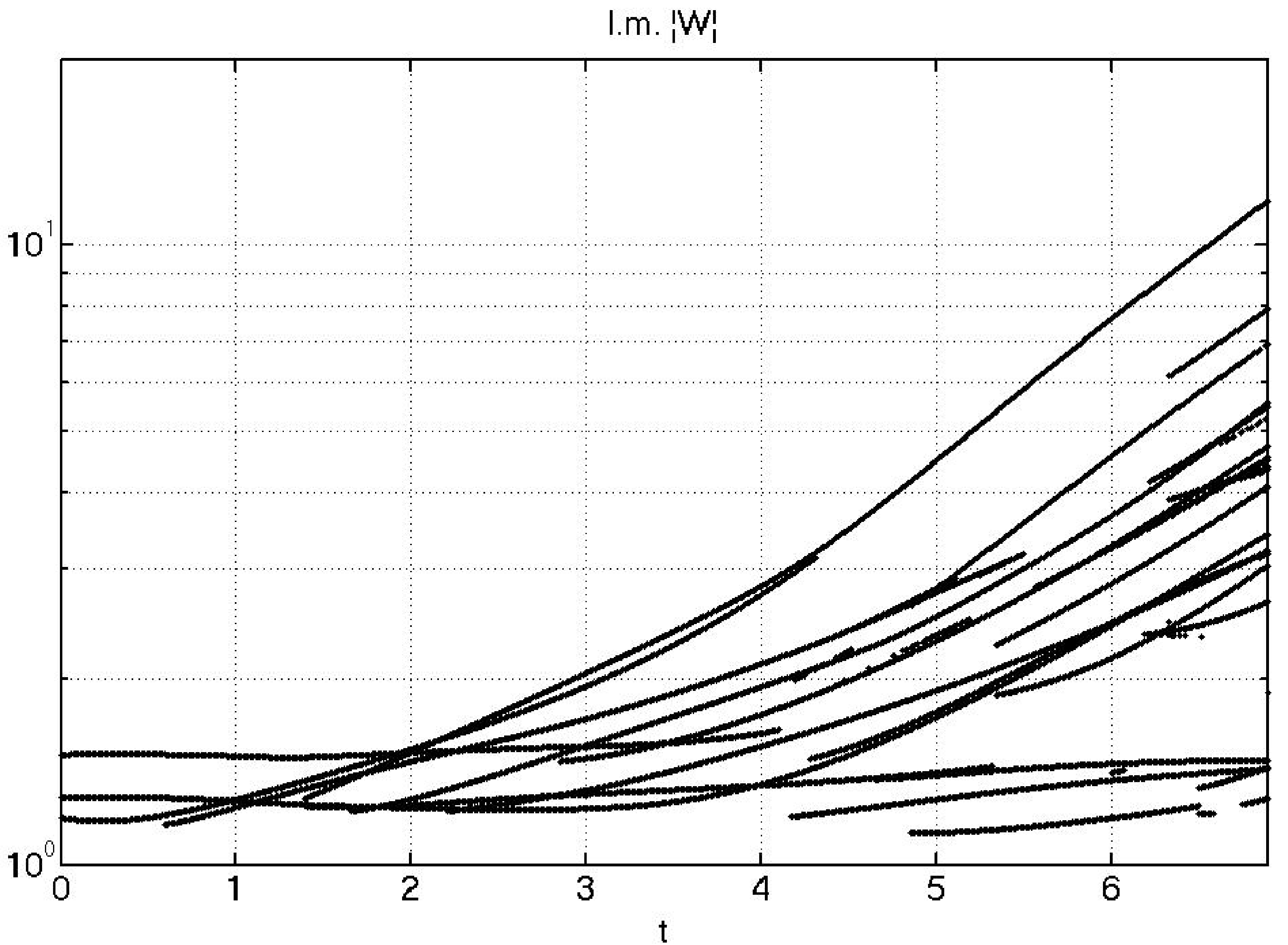

Evolution of local maximums of vorticity field.

3. Simulation results.

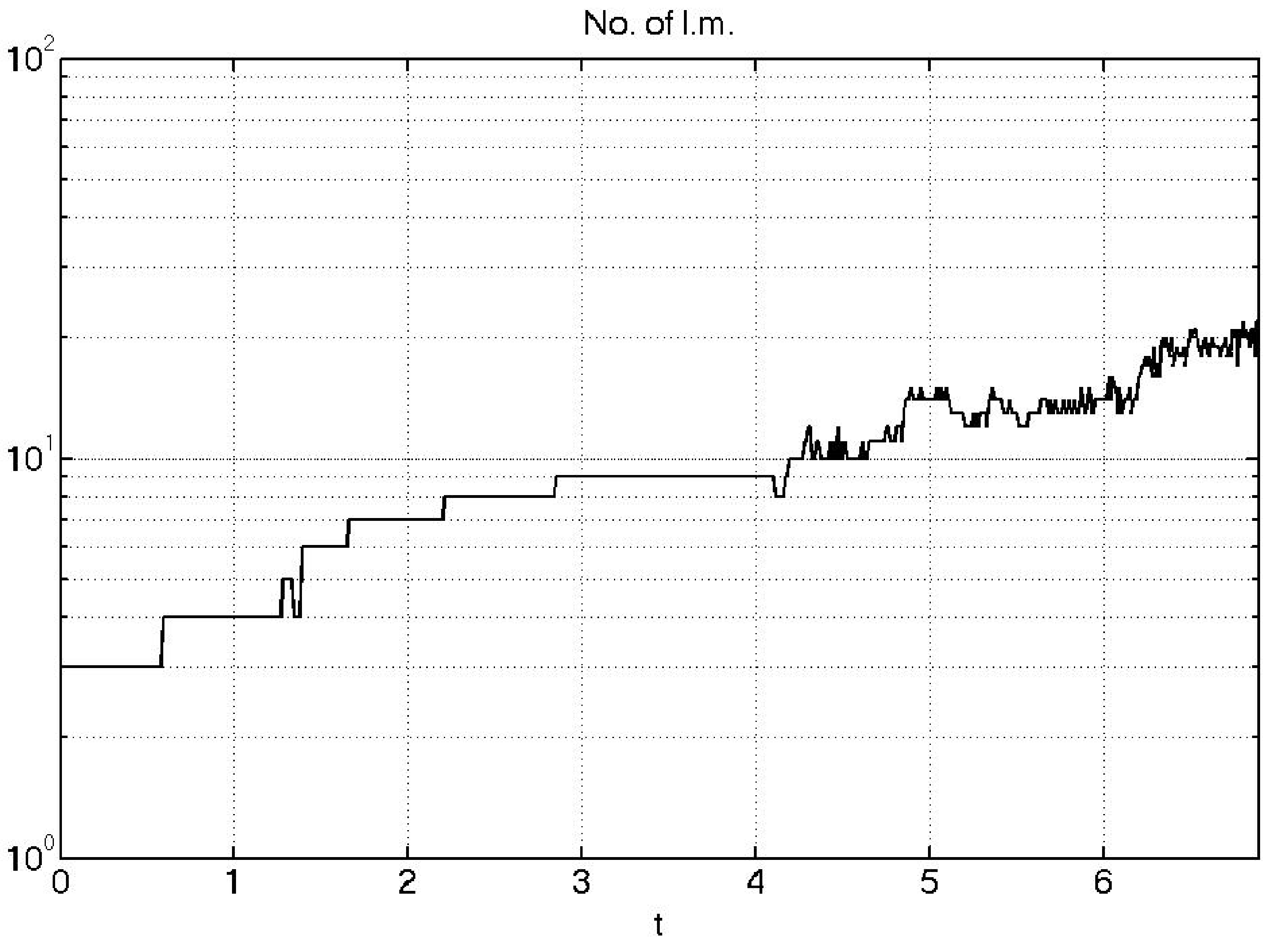

Evolution of the total number of local maximums of vorticity field.

3. Simulation results.

Let us suppose that at the point $\mathbf{r_0}$ we have local maximum of vorticity field. Then in the vicinity of this point vorticity can be expanded in Taylor series as

$$|\omega(\mathbf{r})| \approx |\omega(\mathbf{r}_0)| + \frac{1}{2}(\mathbf{r}-\mathbf{r}_0)\mathbf{H}(\mathbf{r}-\mathbf{r}_0)^T + o(|\mathbf{r}-\mathbf{r}_0|^2),$$

where H is symmetric negatively defined Hessian matrix,

$$H_{ij} = \frac{\partial^2 |\omega(\mathbf{r})|}{\partial x_i \partial x_j}\Big|_{\mathbf{r}=\mathbf{r}_0}, \quad i, j = x, y, z.$$

The matrix **H** has three negative eigenvalues $\boldsymbol{\lambda_1 \le \lambda_2 \le \lambda_3 \le 0}$ corresponding to three orthonormal eigenvectors $\{\mathbf{w_1}, \mathbf{w_2}, \mathbf{w_3}\}$. It is convenient to use the new coordinates in this orthonormal basis as

$$\mathbf{r} = \mathbf{r}_0 + u_1\mathbf{w}_1 + u_2\mathbf{w}_2 + u_3\mathbf{w}_3,$$

which brings the quadratic term in Taylor expansion to diagonal form,

$$|\omega(\mathbf{r})| \approx |\omega(\mathbf{r}_0)| + \frac{1}{2}\left(\lambda_1 u_1^2 + \lambda_2 u_2^2 + \lambda_3 u_3^2\right) + o(|\mathbf{r}-\mathbf{r}_0|^2).$$

In the new coordinates $\mathbf{u = (u_1, u_2, u_3)}$, the vorticity maximum corresponds to the origin and the singularity region is rotated to align the principal axes of its quadratic approximation. As will be shown below, in the new coordinate system the singularity region represents a thin (pancake) structure, where the thickness (along u_1 -axis) decreases much faster than its width along the u_2 and u_3 axes.

3. Simulation results.

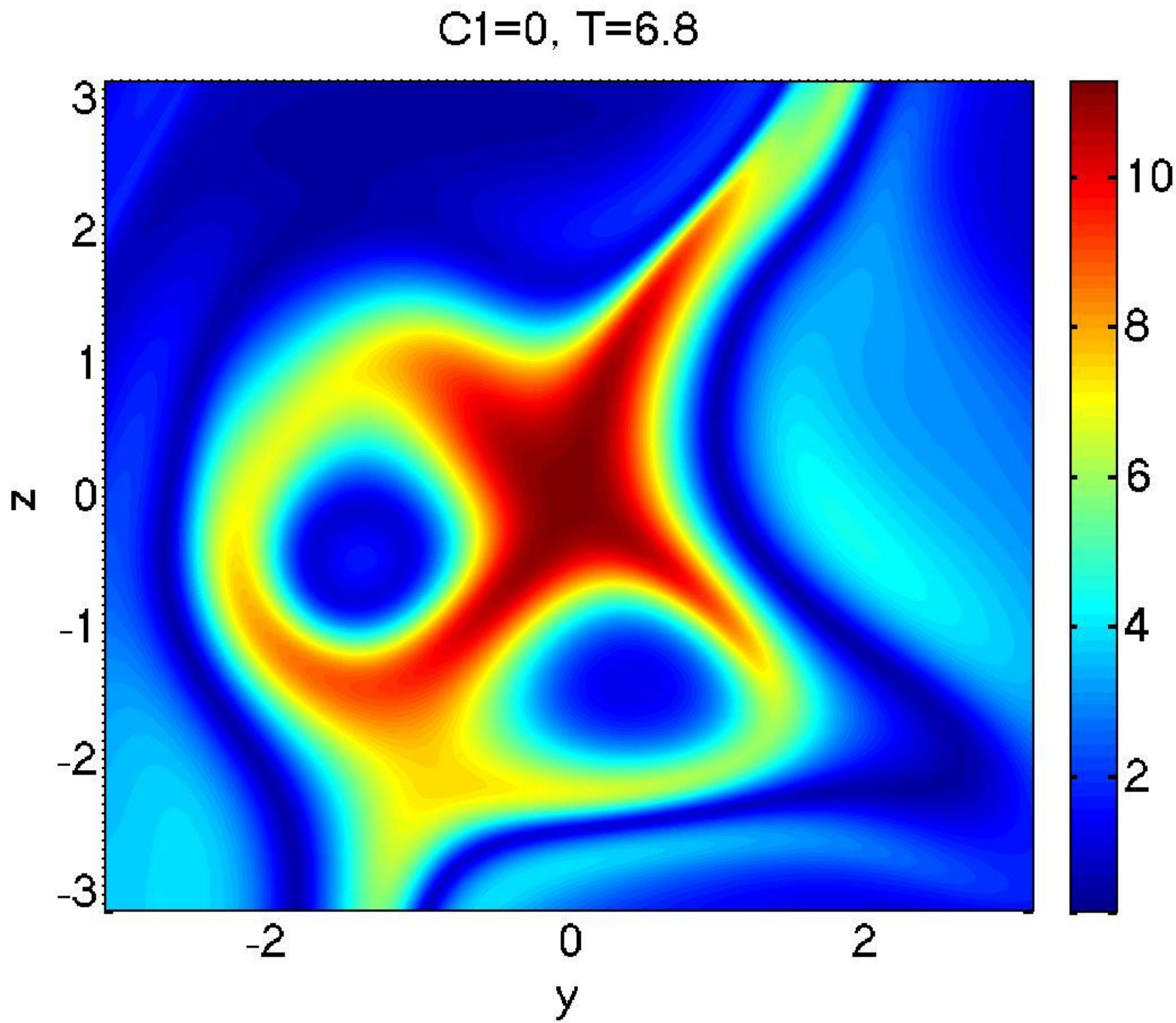

3. Simulation results.

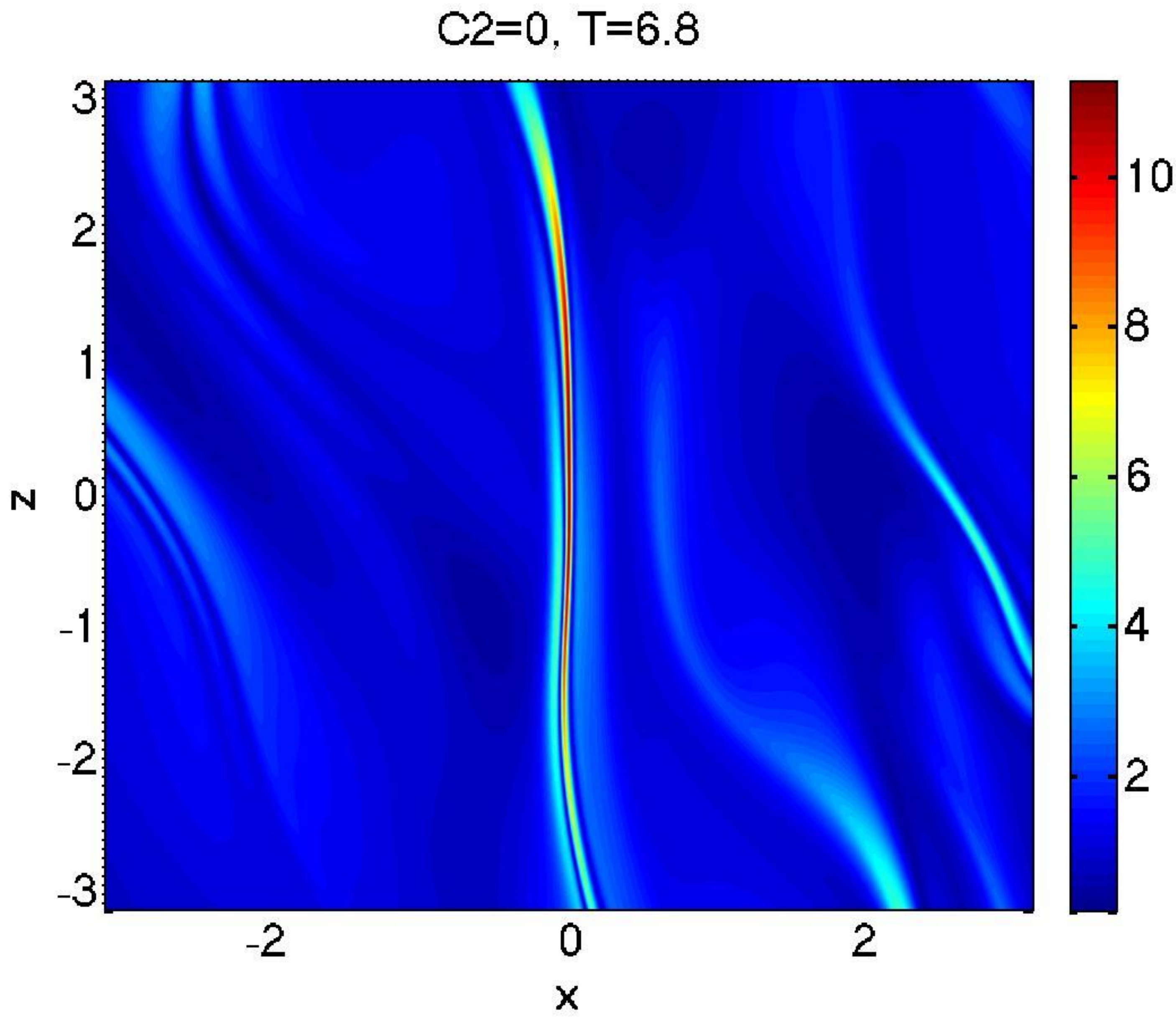

3. Simulation results.

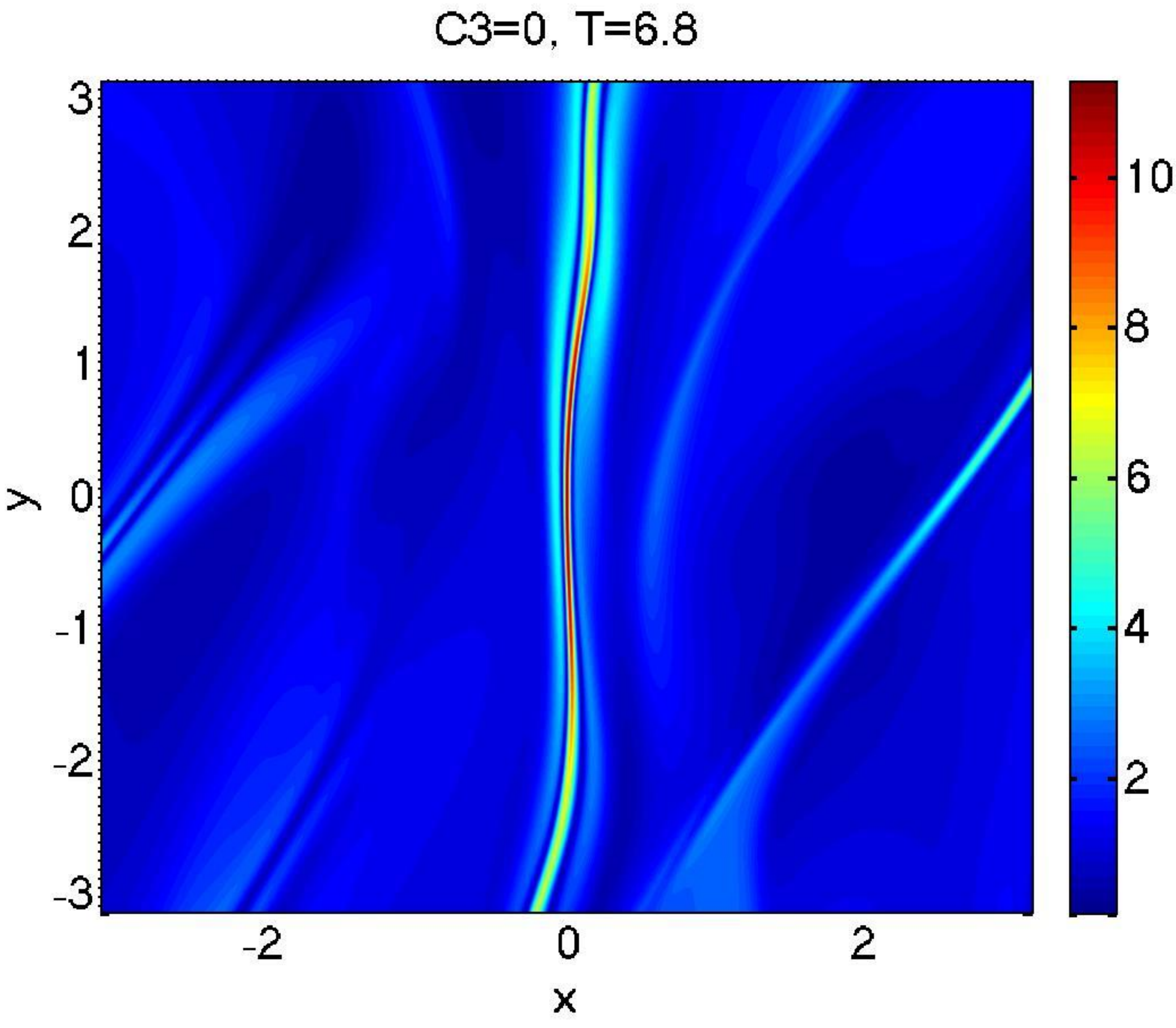

3. Simulation results.

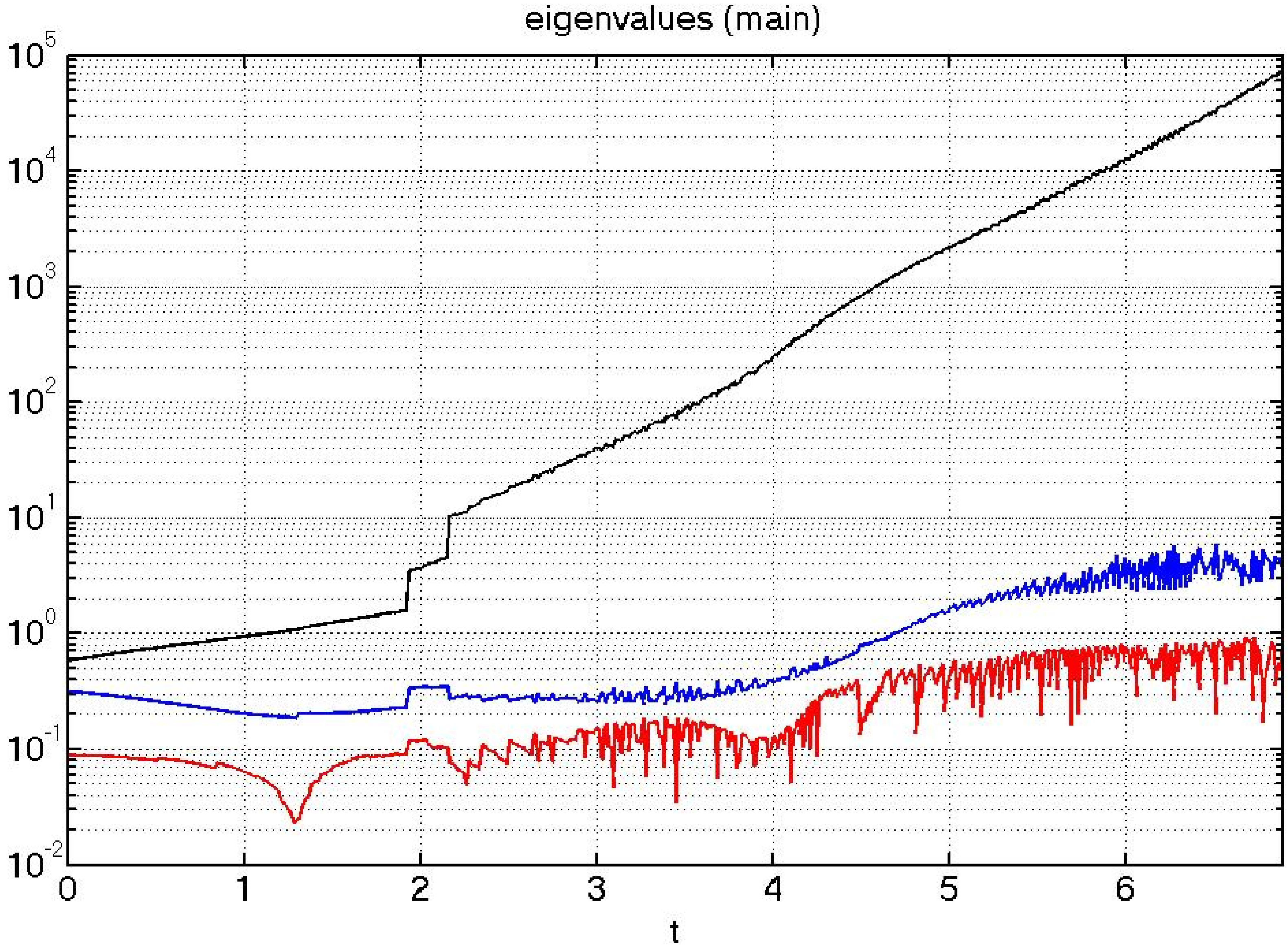

Evolution of eigenvalues for the Hessian matrix (global maximum).

3. Simulation results.

According to the Taylor series in the new coordinates, the singularity region near the vorticity local maximum possesses three effective spatial dimensions given by

$$\ell_i = \sqrt{\frac{|\omega(\mathbf{r}_0)|}{-\lambda_i}}, \quad i = 1, 2, 3.$$

Each of these dimensions corresponds to the decay of vorticity by half along the respective axis. The evolution of these dimensions for the global maximum is shown below. The smallest characteristic scale $\boldsymbol{\lambda}_1$ (thickness) decays nearly exponentially with time by almost two orders of magnitude up to the scale of about **10** $\Delta\mathbf{x}$, where $\Delta\mathbf{x}$ is the spacial grid size. The other two characteristic scales $\boldsymbol{\lambda}_2$ and $\boldsymbol{\lambda}_3$ do not change substantially.

3. Simulation results.

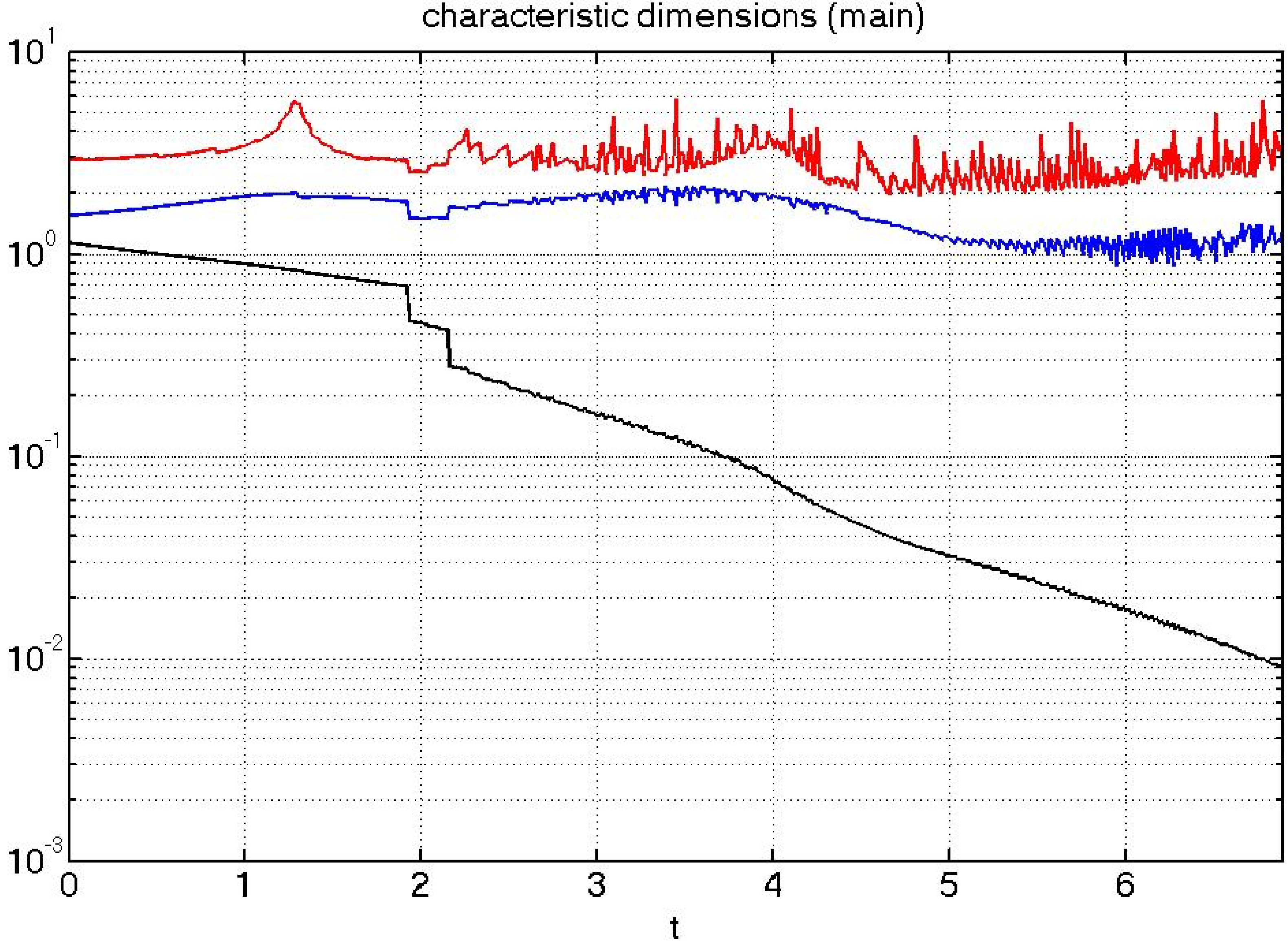

Evolution of the characteristic scales of the singularity (global maximum).

3. Simulation results.

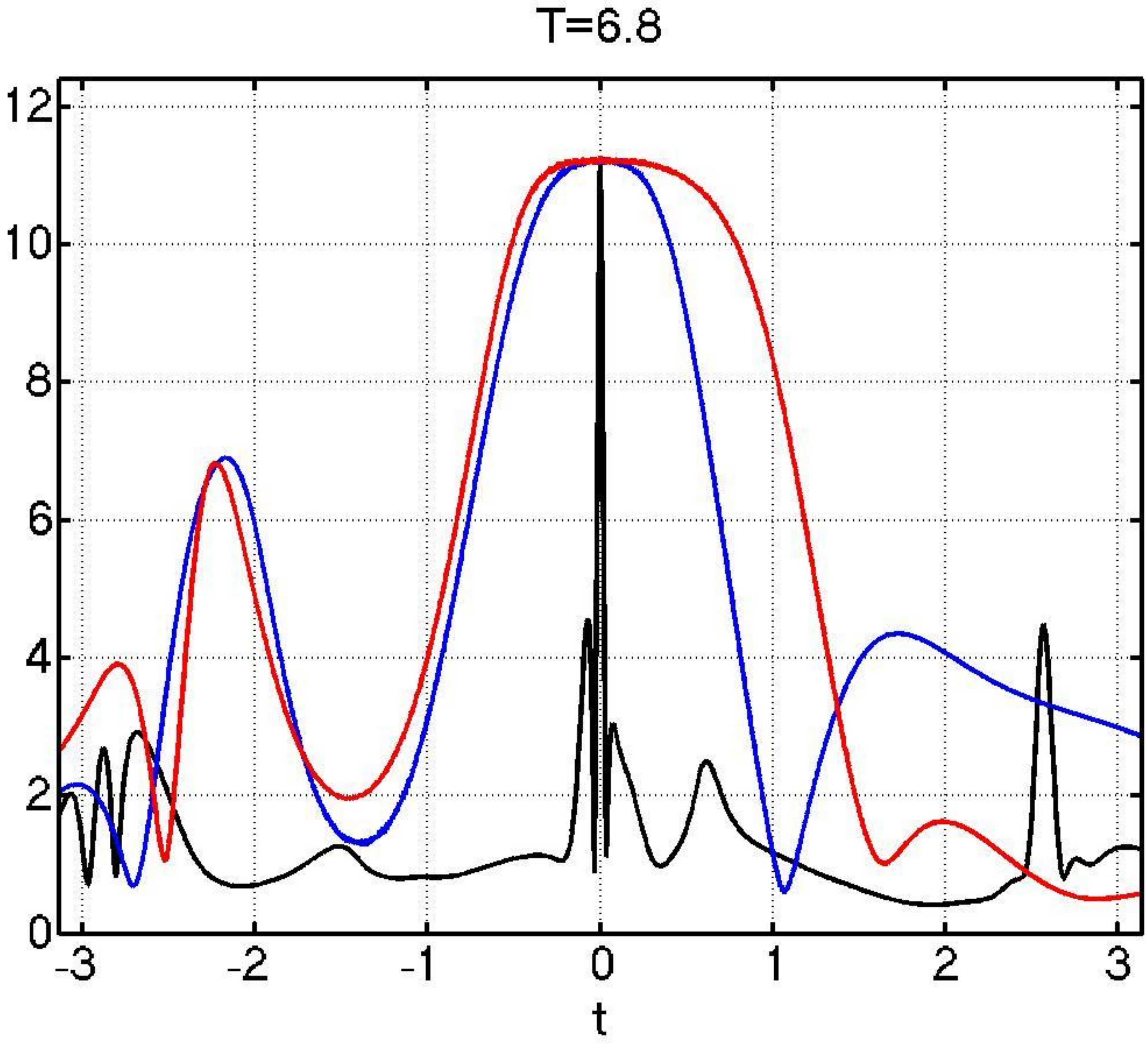

Vorticity field along the principal axis (global maximum).

3. Simulation results.

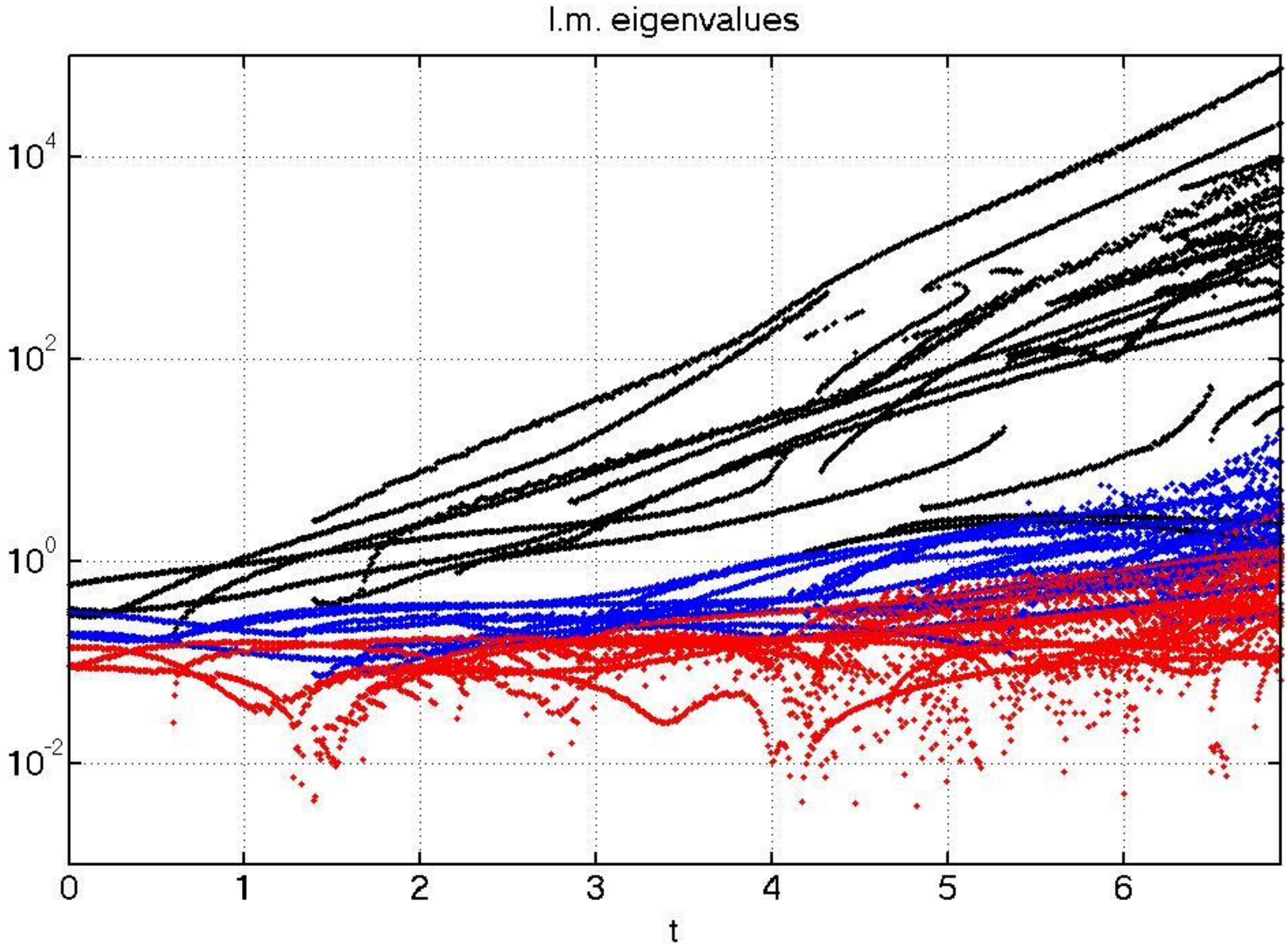

Evolution of eigenvalues for the Hessian matrix (local maximums).

3. Simulation results.

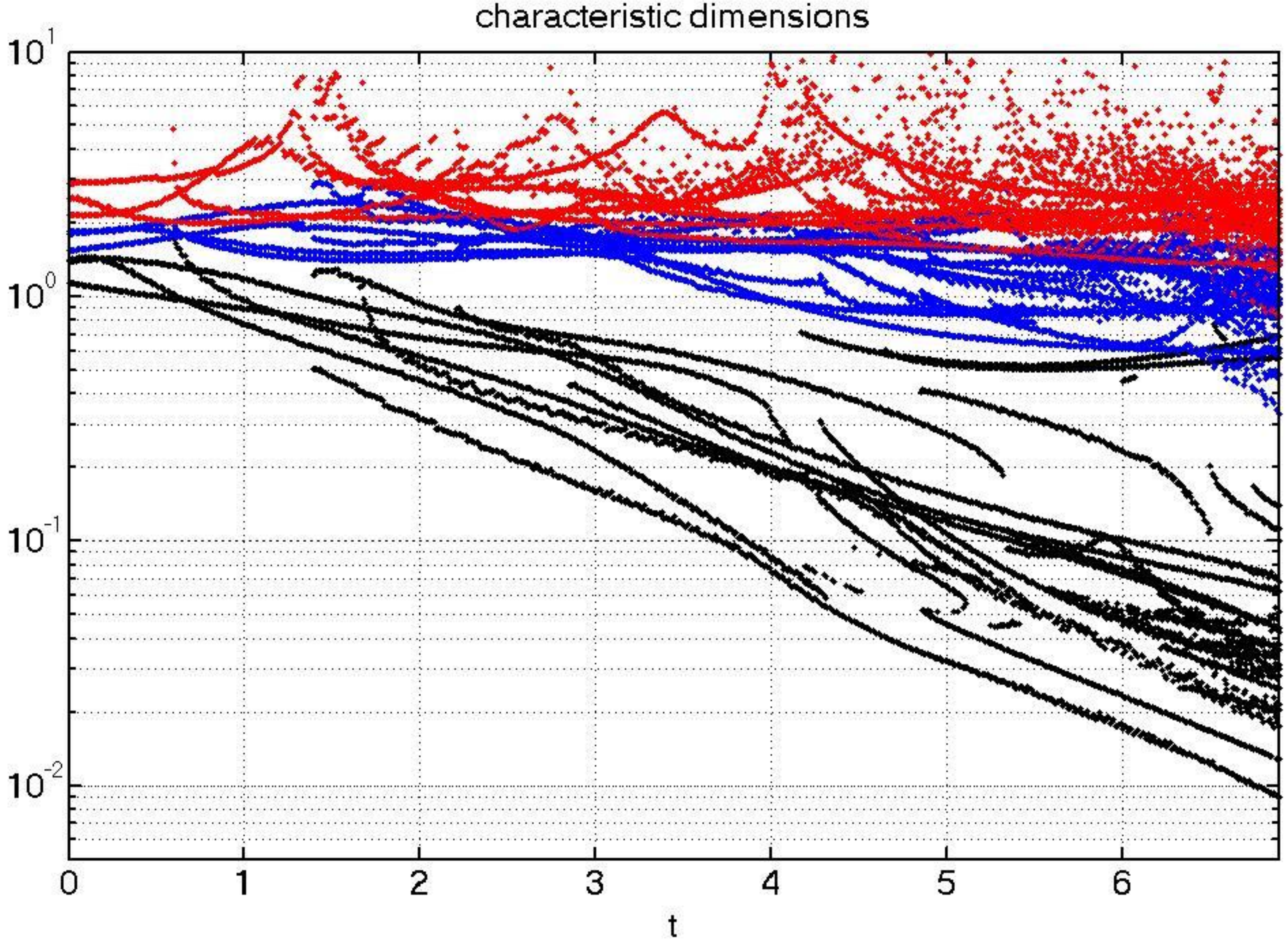

Evolution of the characteristic scales of the singularities (local maximums).

3. Simulation results.

Preliminary conclusions:

(1) At small wavenumbers **k ~ 5-10** we observe the formation of Kolmogorov spectrum:

$$\varepsilon(k,t) \to const \times k^{-5/3}.$$

The spectrum at these wavenumbers becomes “frozen” in time, while the spectrum at larger wavenumbers significantly evolves.

(2) We observe exponential behavior of the singularities: the values of the local maximums of vorticity increase with time exponentially – for all local maximums and roughly with the same increment. All singularities represent pancake structures, quickly compressing in one direction and remaining finite in two other directions. The compression along the width of all pancakes is exponential – for all local maximums and roughly with the same increment.

The main idea, that we think is right, is that these singularities are the sink that absorbs energy from large scales and transfer it to small scales. This sink play the role of viscosity and ensures the formation of Kolmogorov interval.

3. Simulation results.

(1) The spectrum is determined by the main singularity, that therefore itself evolves according to Kolmogorov laws.

(2) All our singularities are in fact correlated and their distribution plays the main role in shaping the Kolmogorov interval in the spectrum.

For each of the local maximums we know its characteristics scales, that we find from the quadratic approximation:

$$\ell_i = \sqrt{|\omega(\mathbf{r}_0)| / |\lambda_i|}, \quad i = 1, 2, 3, \quad \ell_1 << \ell_2 \sim \ell_3.$$

Therefore, we can assign to each maximum its characteristic width in k-space:

$$\delta k = 1/\ell_1.$$

Now we can check, is there any dependence of local maximum value |**ω**| on its characteristic width in k-space. In case of Kolmogorov spectrum we would have

$$|\omega| \sim \delta k^{2/3}.$$

At every point of time each of the local maximums represents a point in coordinates **(δk, |ω|)**. When we “switch time on”, this point starts to move. And if this point moves along the 2/3-line (log-log scale), then this means that such local maximum develops according to Kolmogorov law.

3. Simulation results.

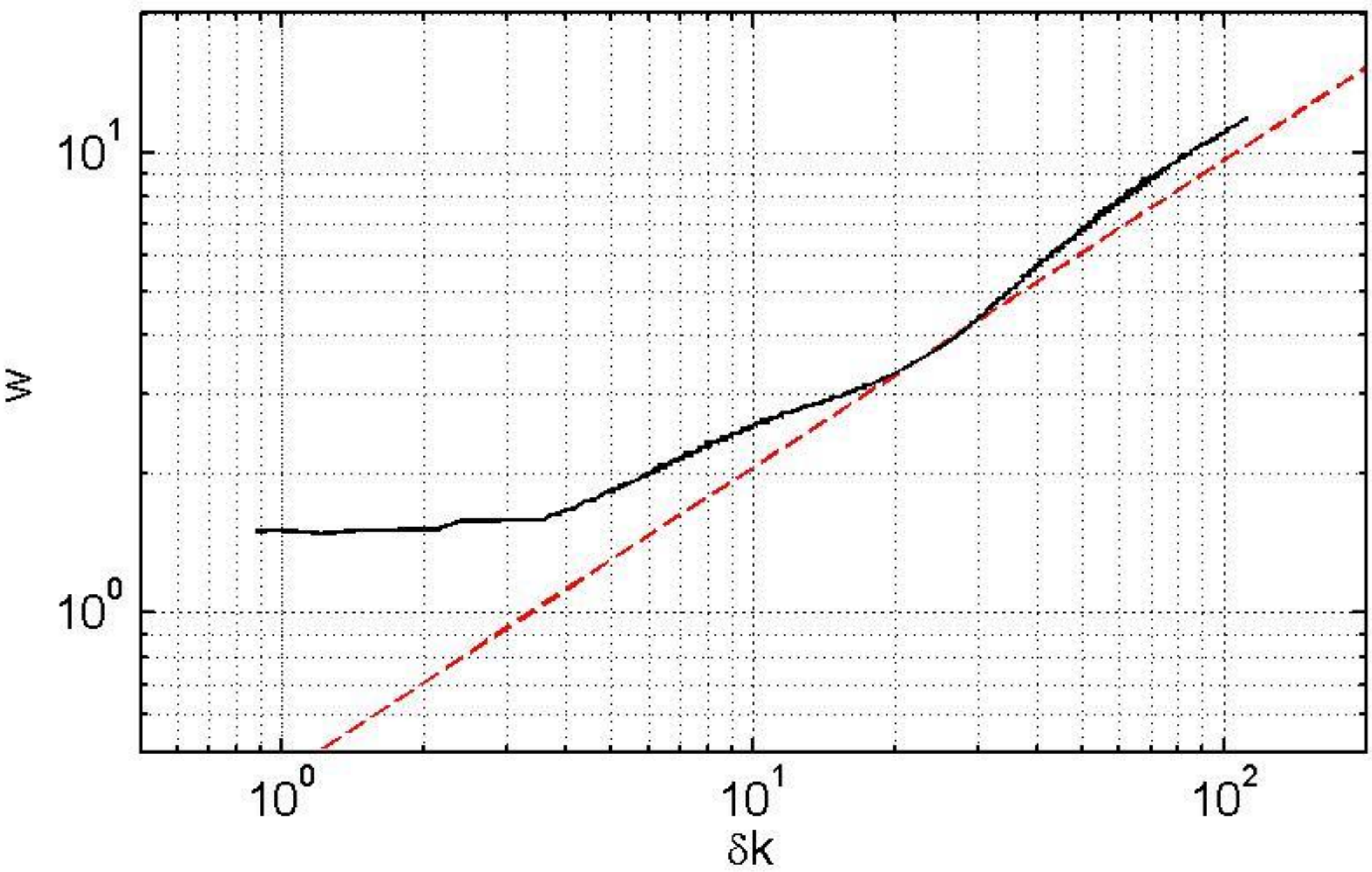

Dependence between the value of the local maximum and its characteristic width in k-space (global maximum).

3. Simulation results.

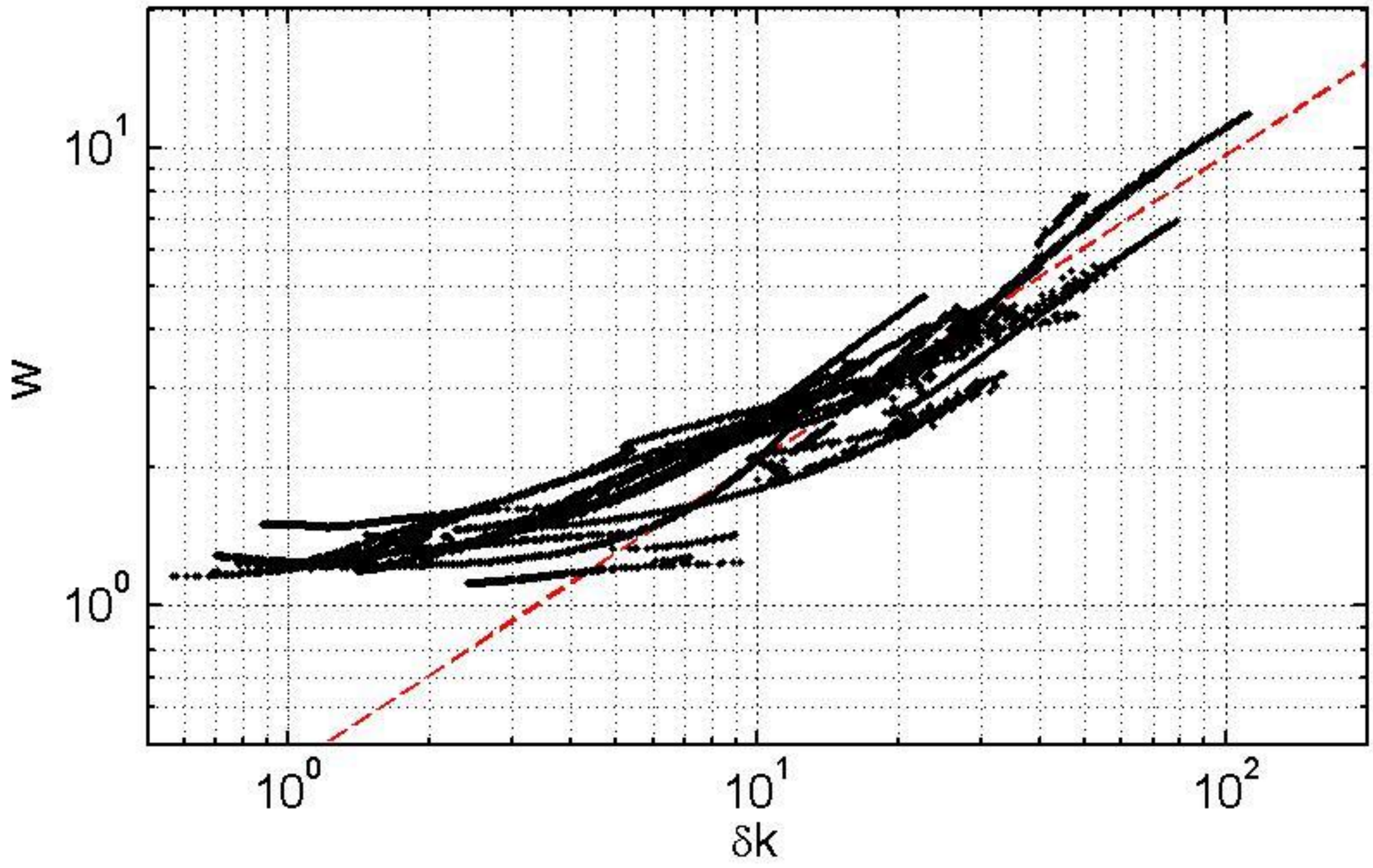

The prefactors for our local maximums in the above equation are close to each over.

$$|\omega| \to C\delta k^{2/3}.$$

3. Simulation results.

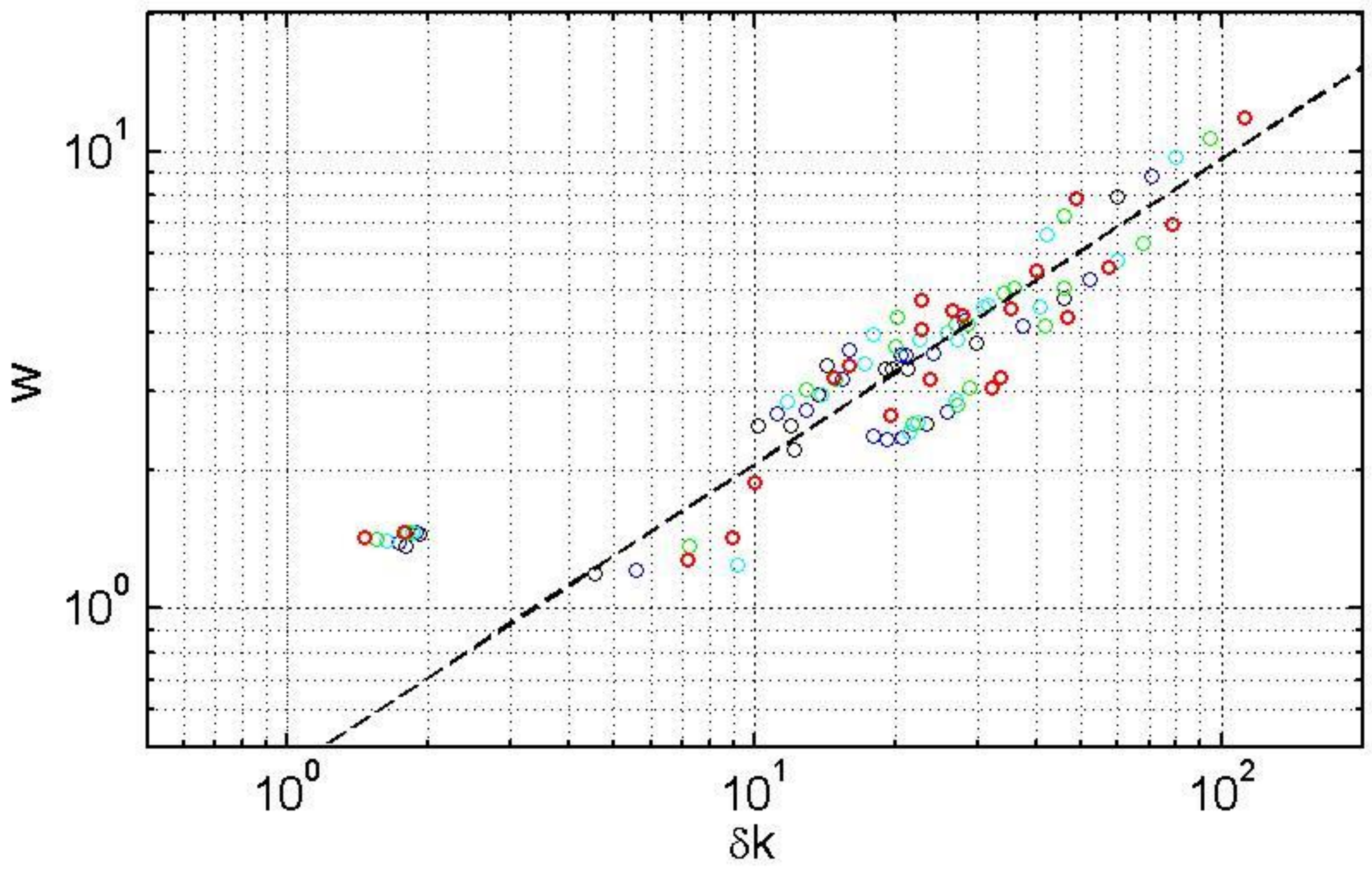

Dependence between the value of the local maximum and its characteristic width in k-space (all local maximums): t = 6.09 (black), t = 6.29 (blue), t = 6.49 (cyan), t = 6.69 (green), t = 6.89 (red).

3. Simulation results.

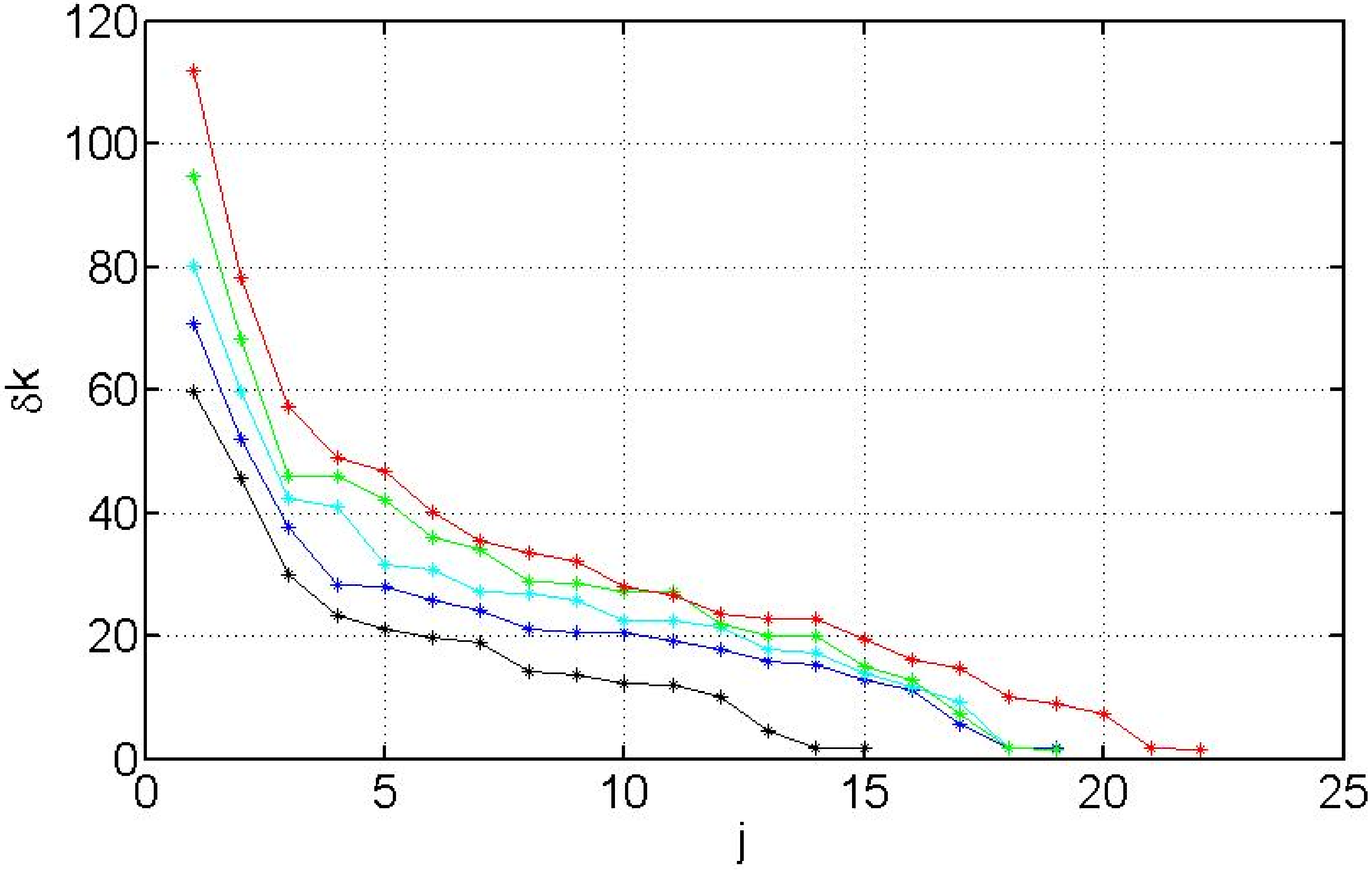

Dependence between the value of the local maximum and its characteristic width in k-space (all local maximums): t = 6.09 (black), t = 6.29 (blue), t = 6.49 (cyan), t = 6.69 (green), t = 6.89 (red).

3. Simulation results.

The “second best” initial data, final grid **1152 x 384 x 2304.**

3. Simulation results.

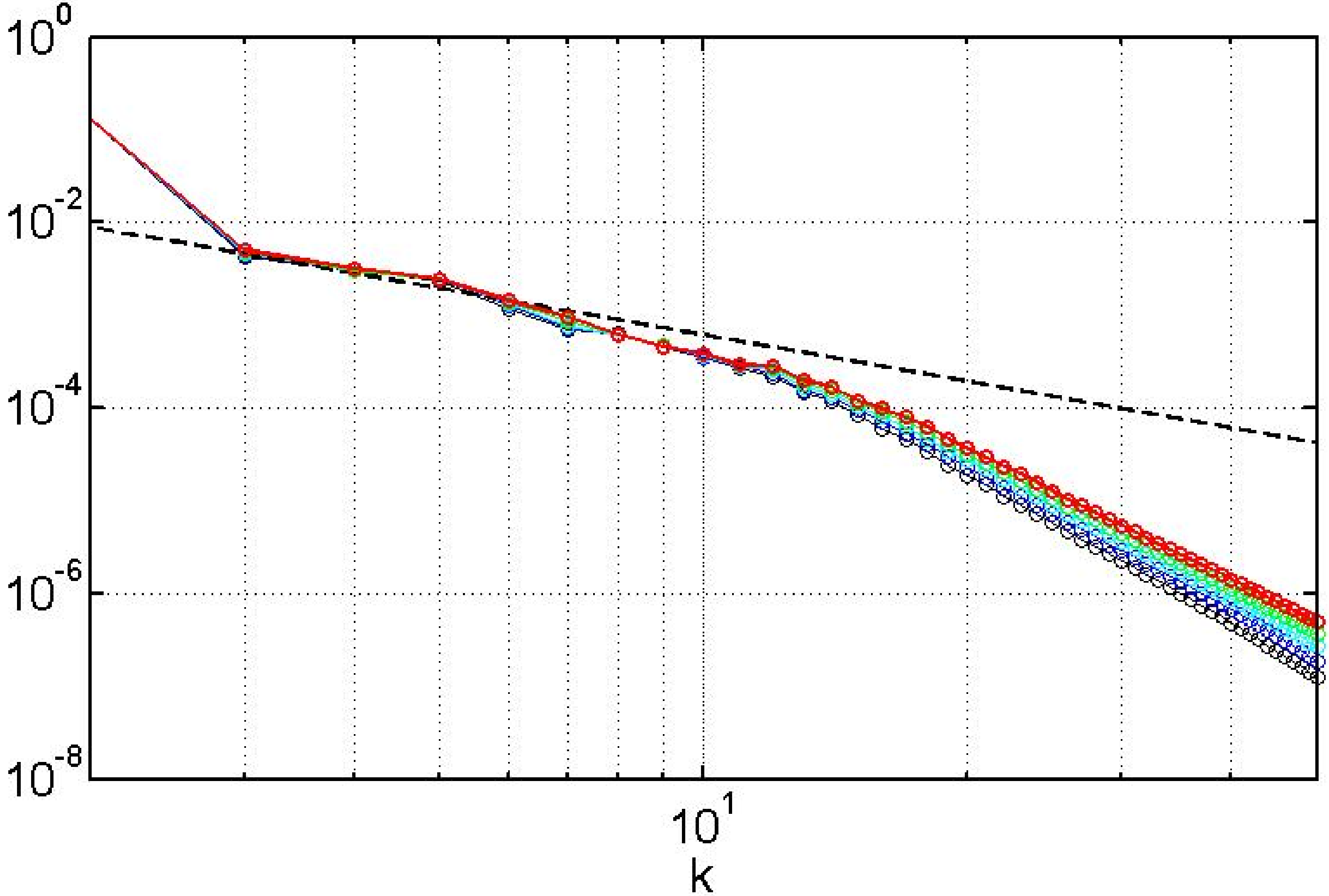

Tendency of the energy spectrum toward the Kolmogorov spectrum: for some of the wavenumbers, **3 ≤ k ≤ 12**, we observe

$$\varepsilon(k,t) \to const \times k^{-5/3}.$$

t = 6.97 (black), t = 7.17 (blue), t = 7.37 (cyan), t = 7.57 (green), t = 7.77 (red).

3. Simulation results.

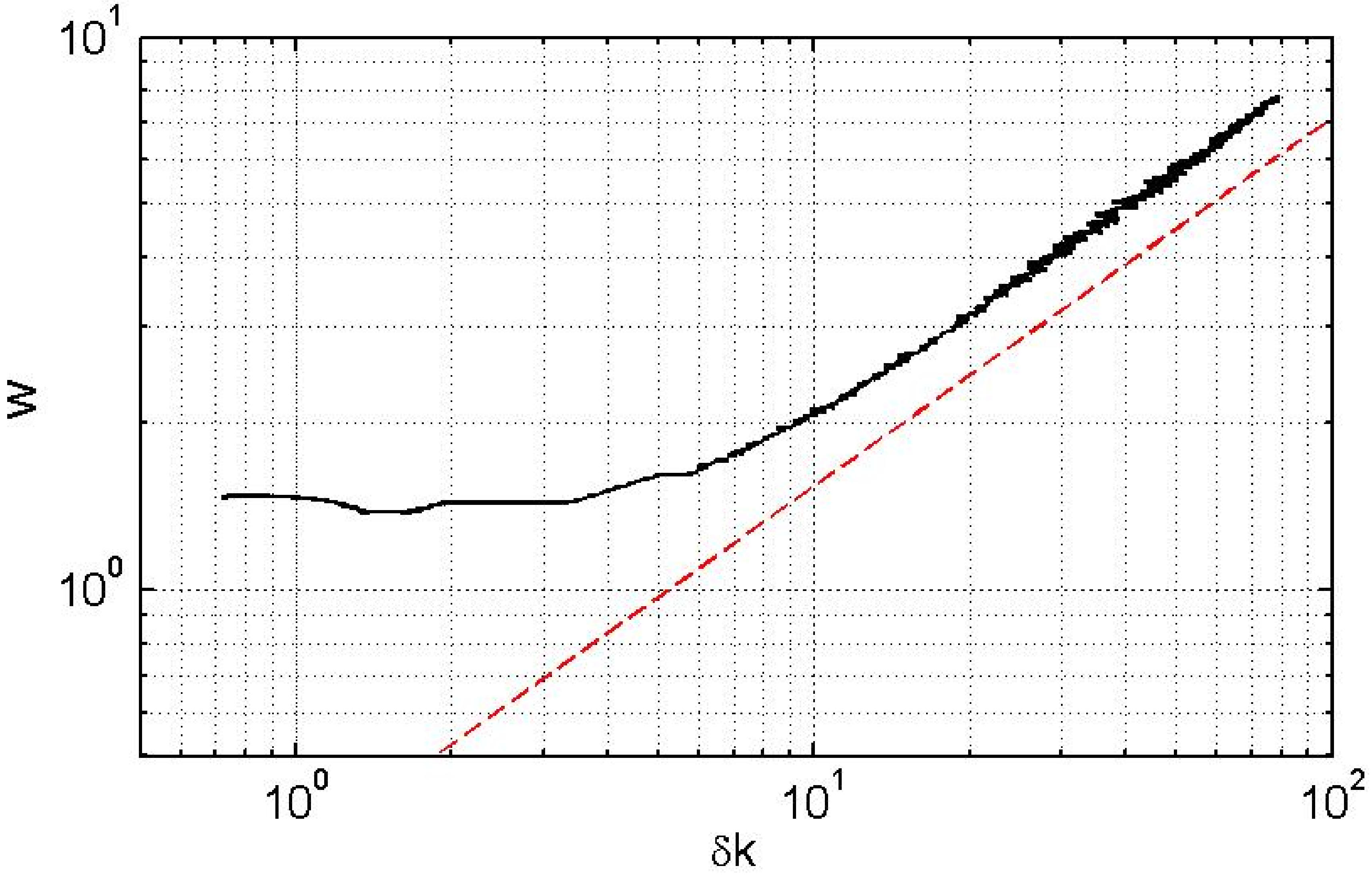

Dependence between the value of the local maximum and its characteristic width in k-space (global maximum).

3. Simulation results.

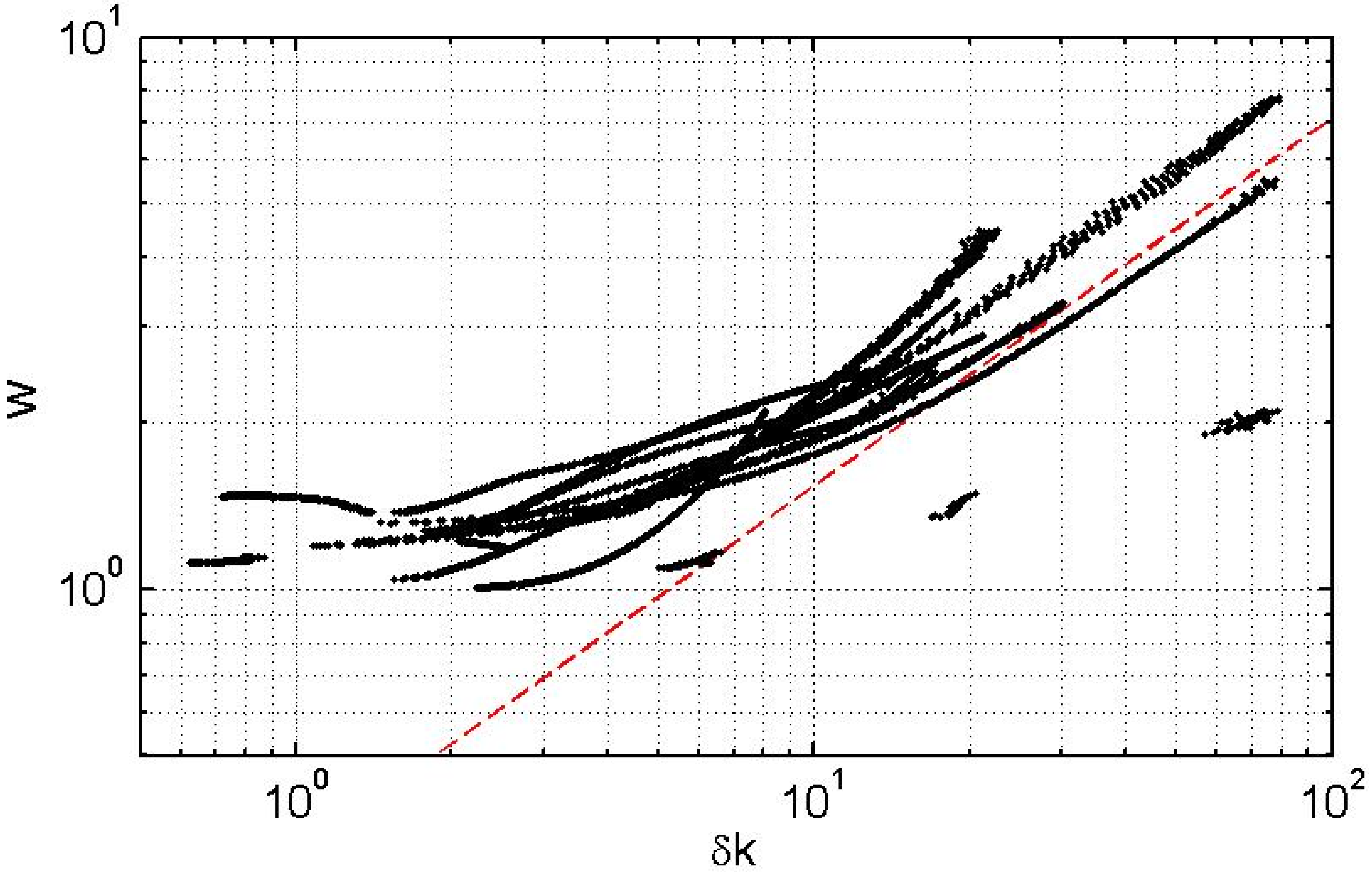

Dependence between the value of the local maximum and its characteristic width in k-space (all local maximums).

3. Simulation results.

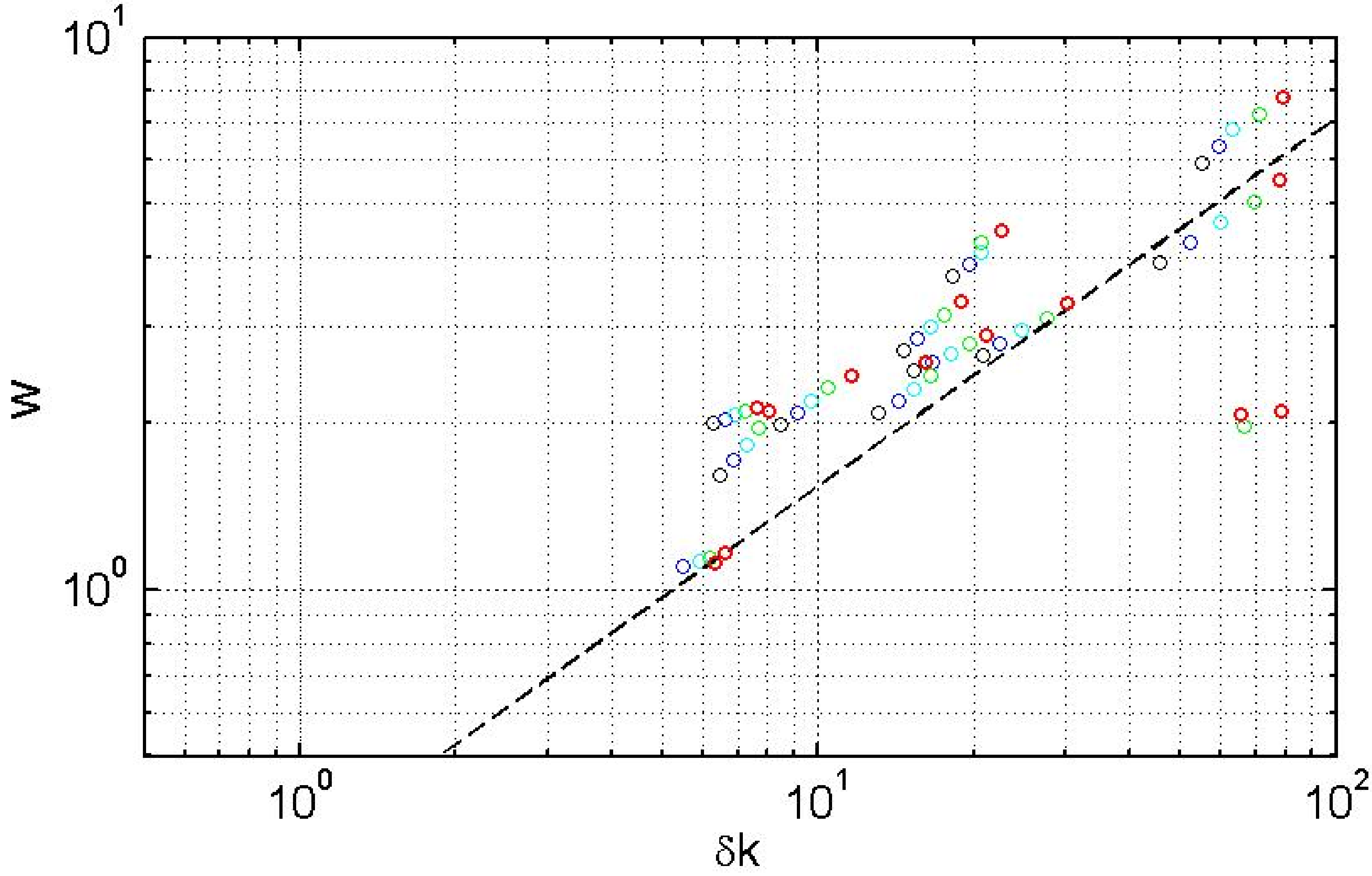

Dependence between the value of the local maximum and its characteristic width in k-space (all local maximums): t = 6.97 (black), t = 7.17 (blue), t = 7.37 (cyan), t = 7.57 (green), t = 7.77 (red).

3. Simulation results.

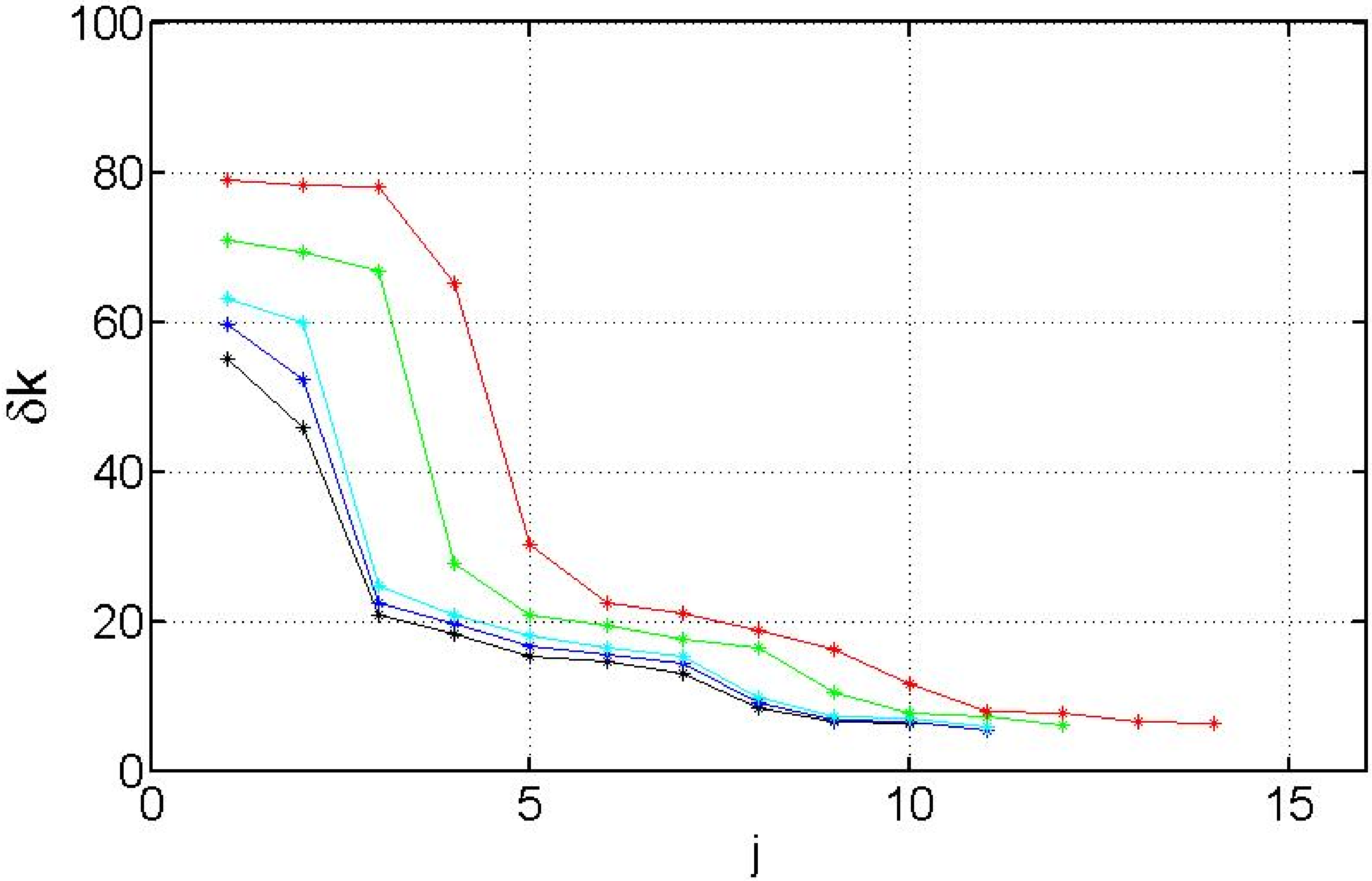

Dependence between the value of the local maximum and its characteristic width in k-space (all local maximums): t = 6.97 (black), t = 7.17 (blue), t = 7.37 (cyan), t = 7.57 (green), t = 7.77 (red).

3. Simulation results.

One of the “general case” initial data, final grid **256 x 486 x 972.**

3. Simulation results.

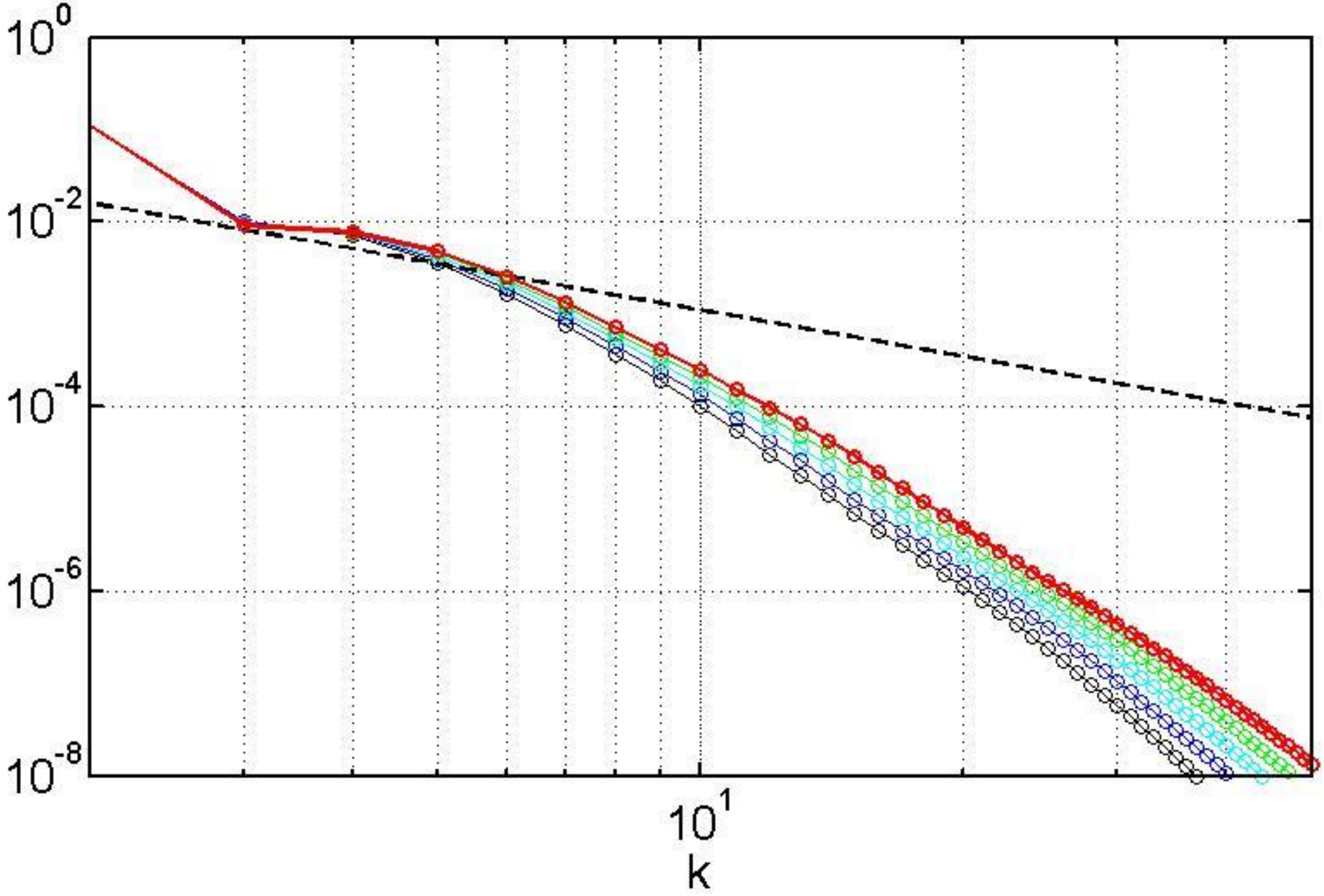

Tendency of the energy spectrum toward the Kolmogorov spectrum: for some of the wavenumbers, **3 ≤ k ≤ 12**, we observe

$$\varepsilon(k,t) \to const \times k^{-5/3}.$$

t = 4.76 (black), t = 4.96 (blue), t = 5.16 (cyan), t = 5.36 (green), t = 5.56 (red).

3. Simulation results.

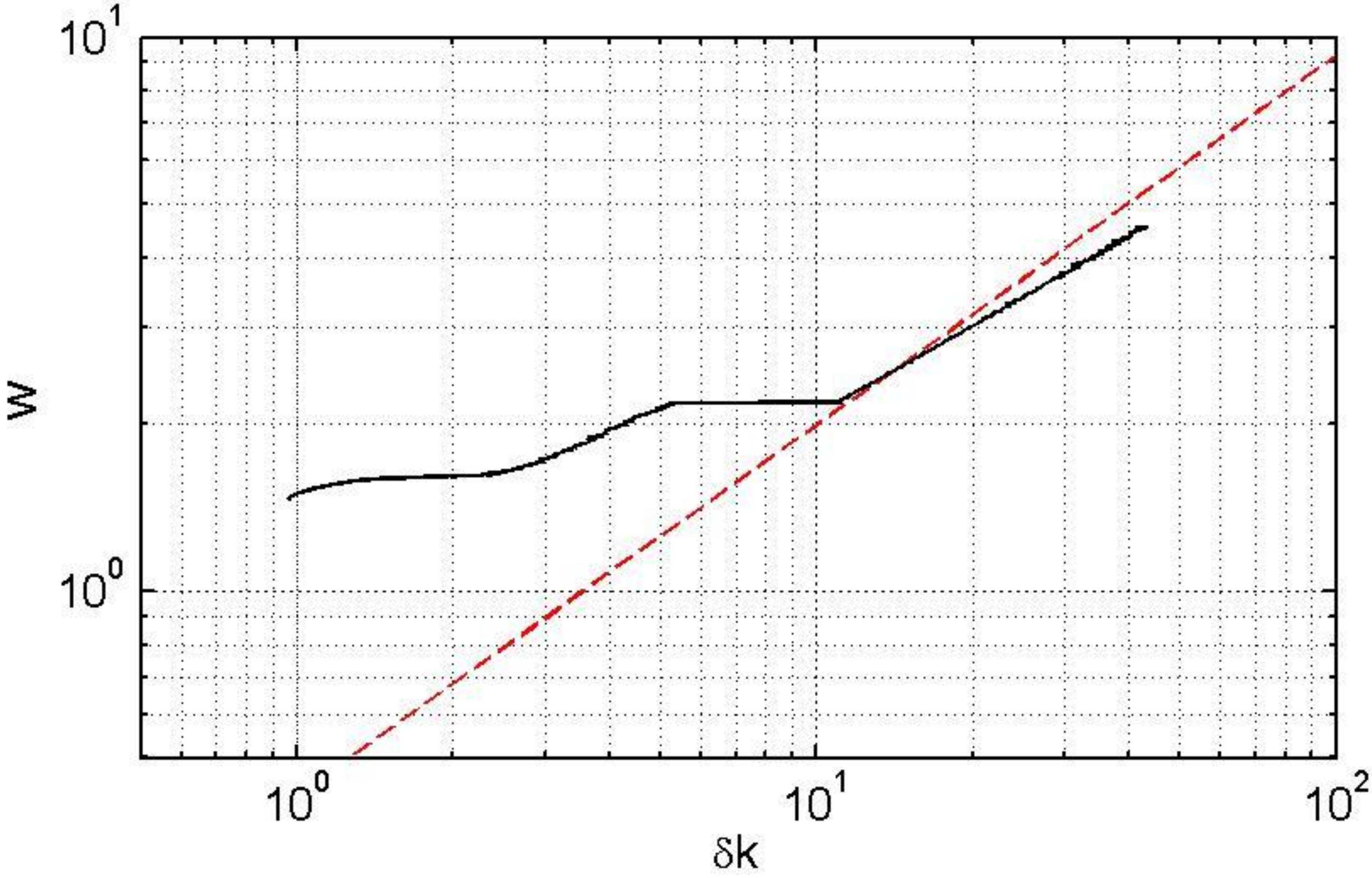

Dependence between the value of the local maximum and its characteristic width in k-space (global maximum).

3. Simulation results.

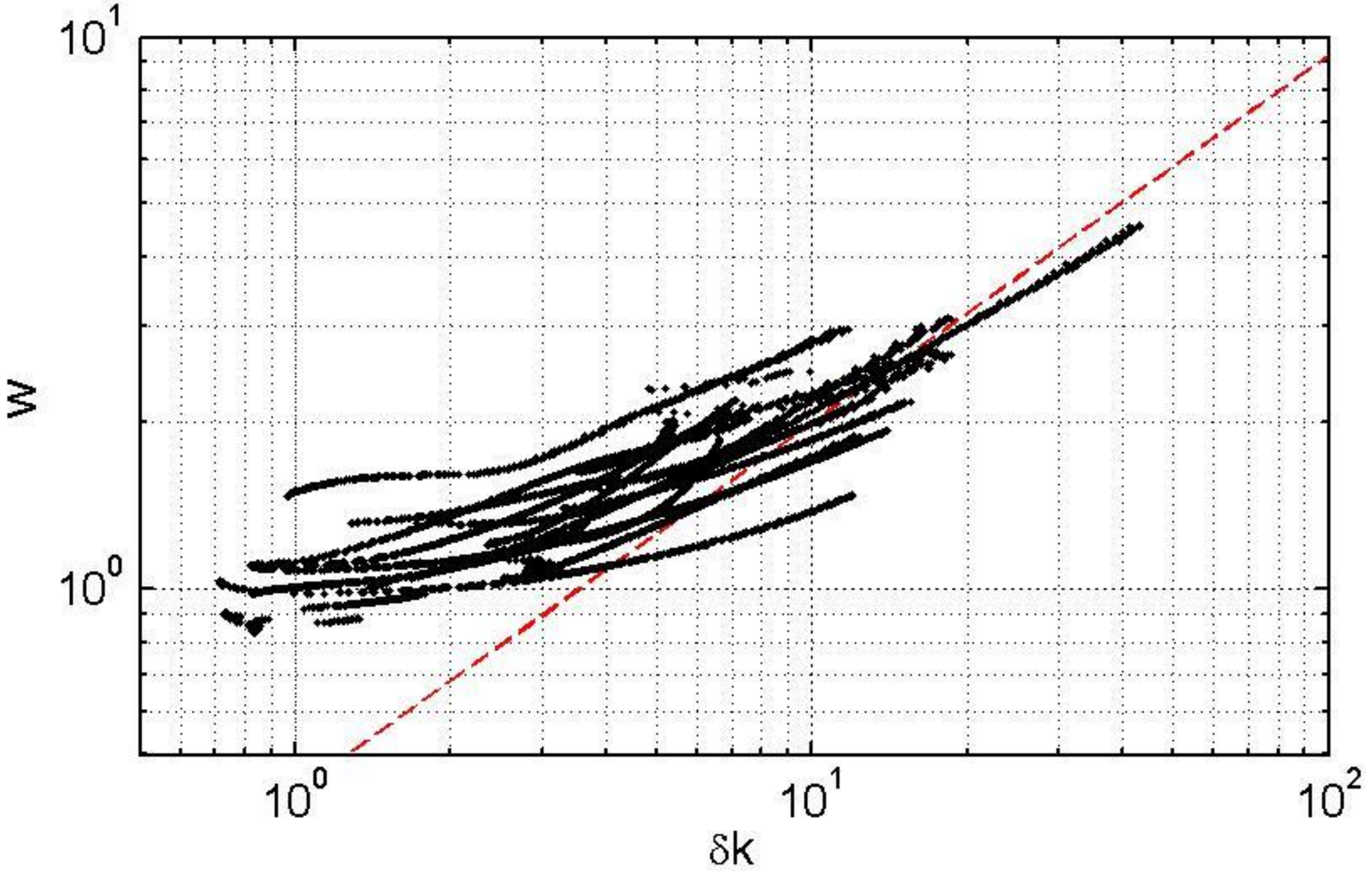

Dependence between the value of the local maximum and its characteristic width in k-space (all local maximums).

3. Simulation results.

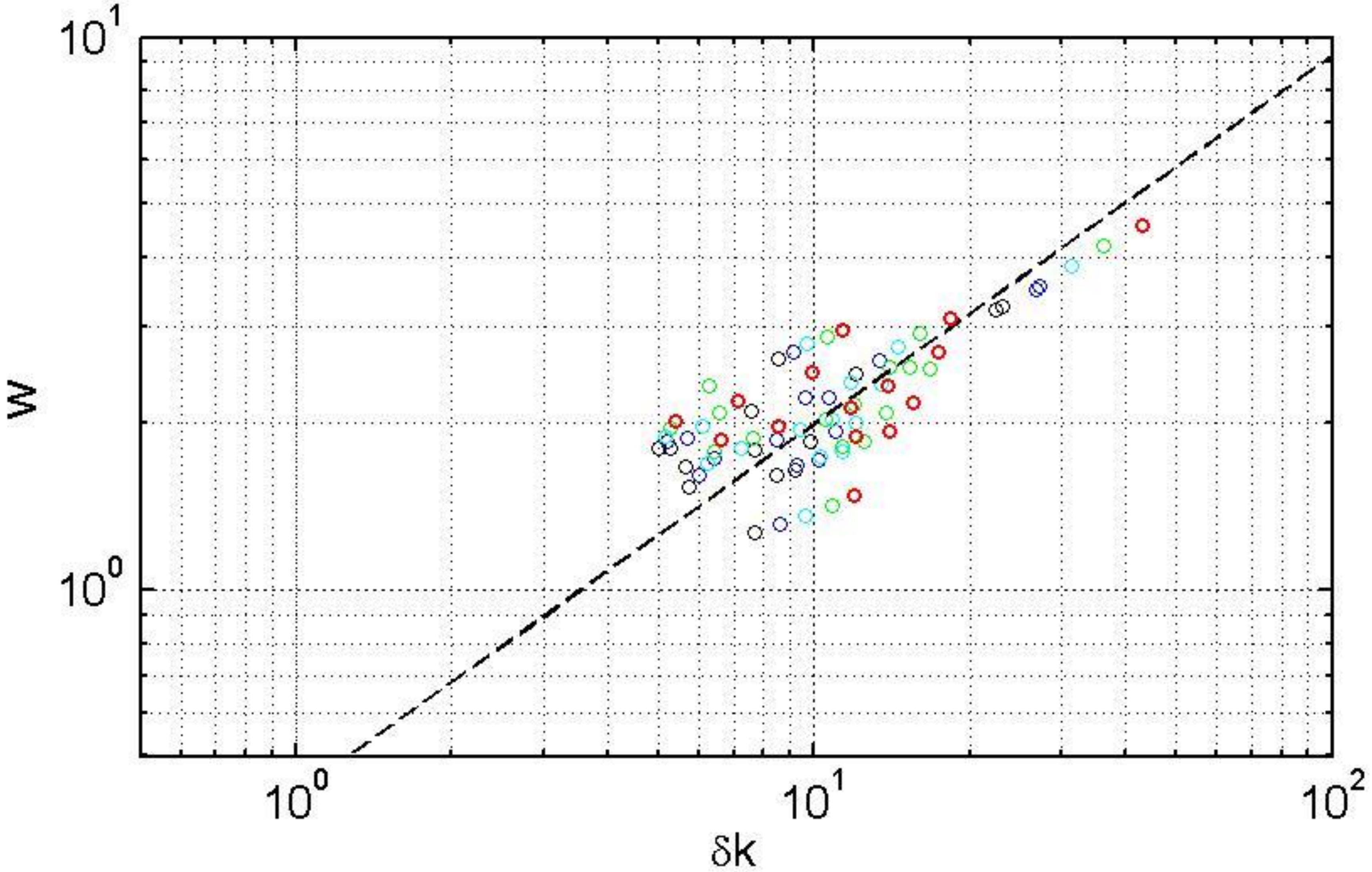

Dependence between the value of the local maximum and its characteristic width in k-space (all local maximums): t = 4.76 (black), t = 4.96 (blue), t = 5.16 (cyan), t = 5.36 (green), t = 5.56 (red).

3. Simulation results.

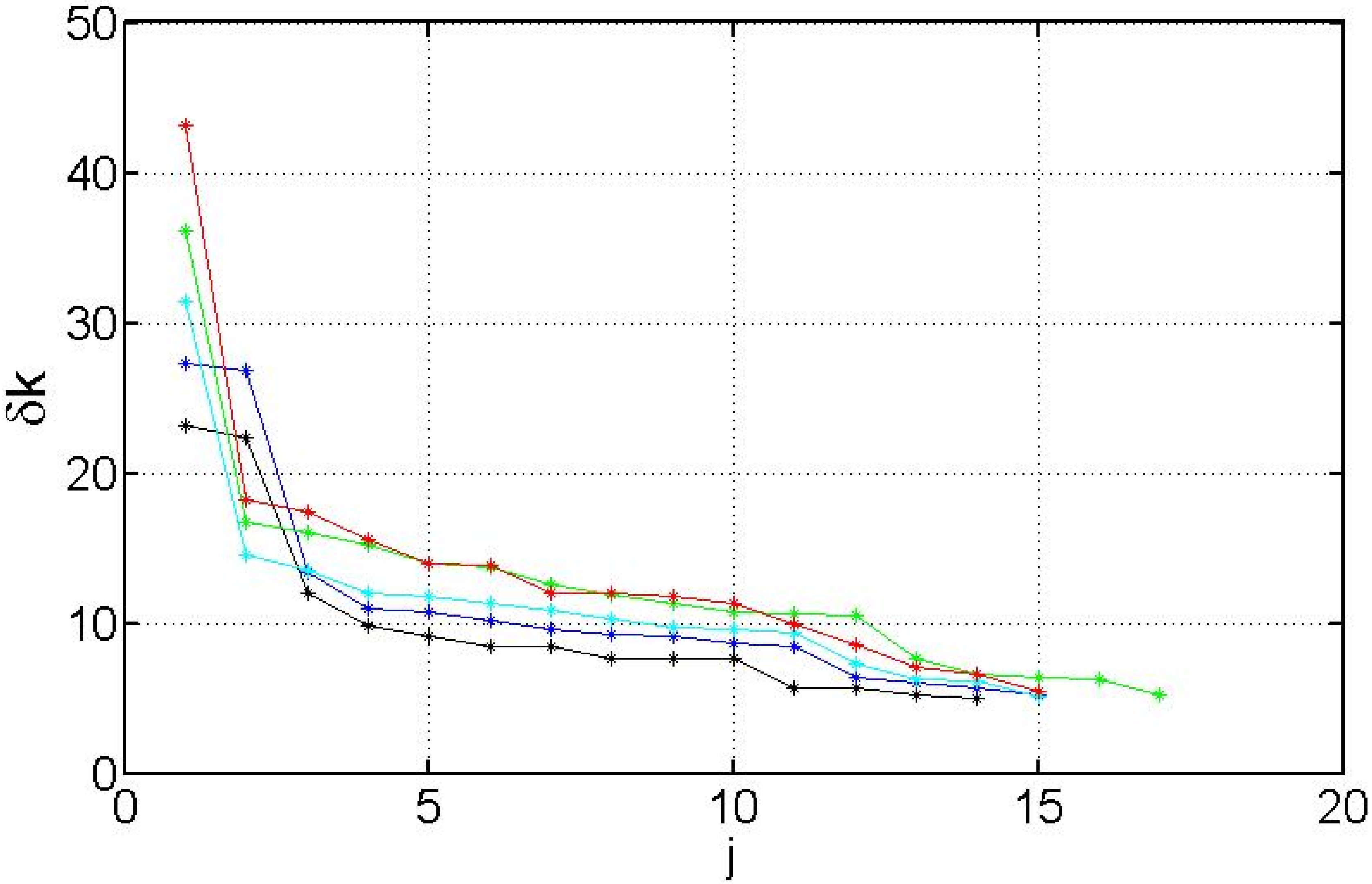

Dependence between the value of the local maximum and its characteristic width in k-space (all local maximums): t = 4.76 (black), t = 4.96 (blue), t = 5.16 (cyan), t = 5.36 (green), t = 5.56 (red).

Thank you for your attention!

3. Simulation results.

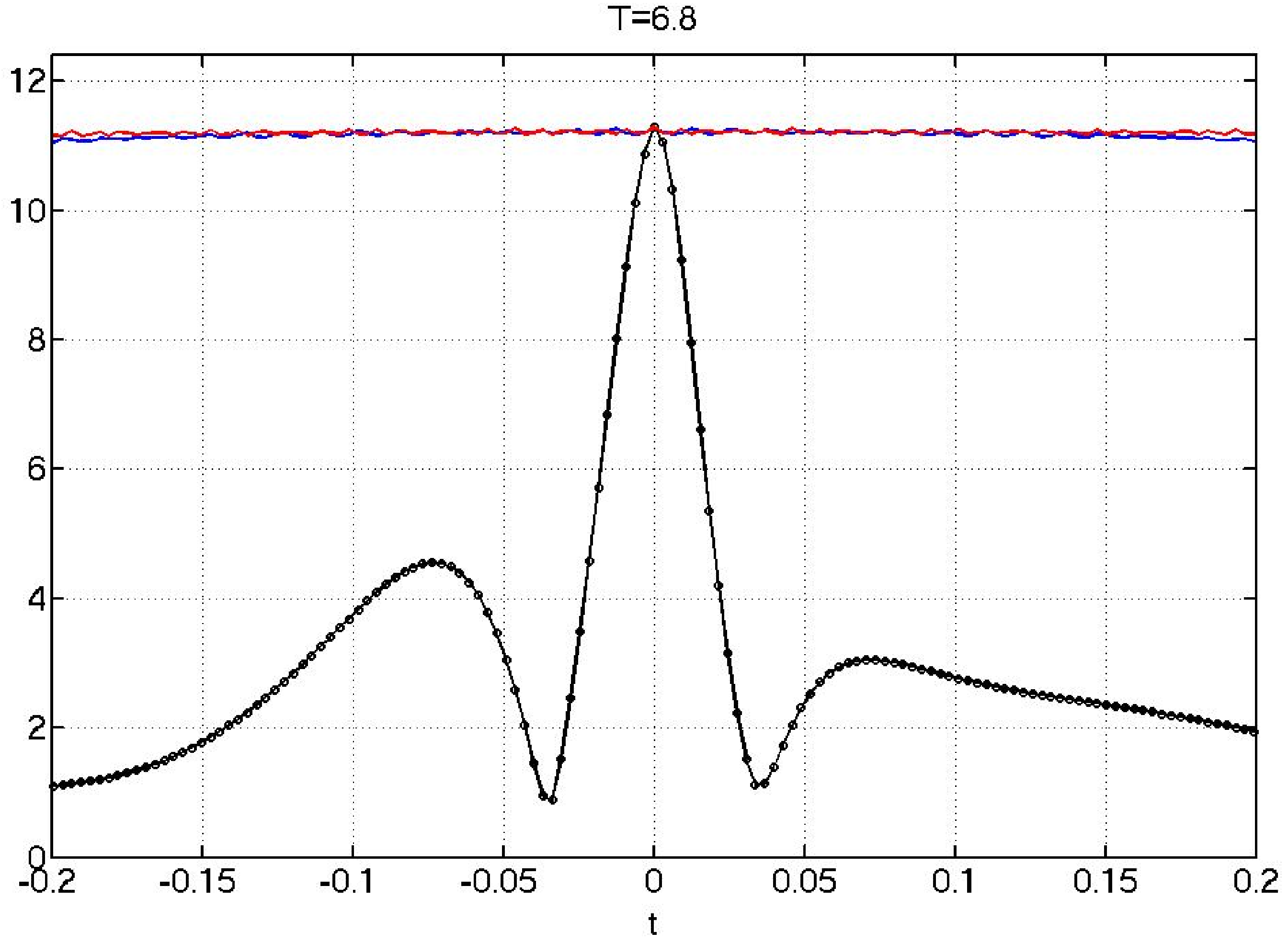

Vorticity field along the principal axis (global maximum).

3. Simulation results.

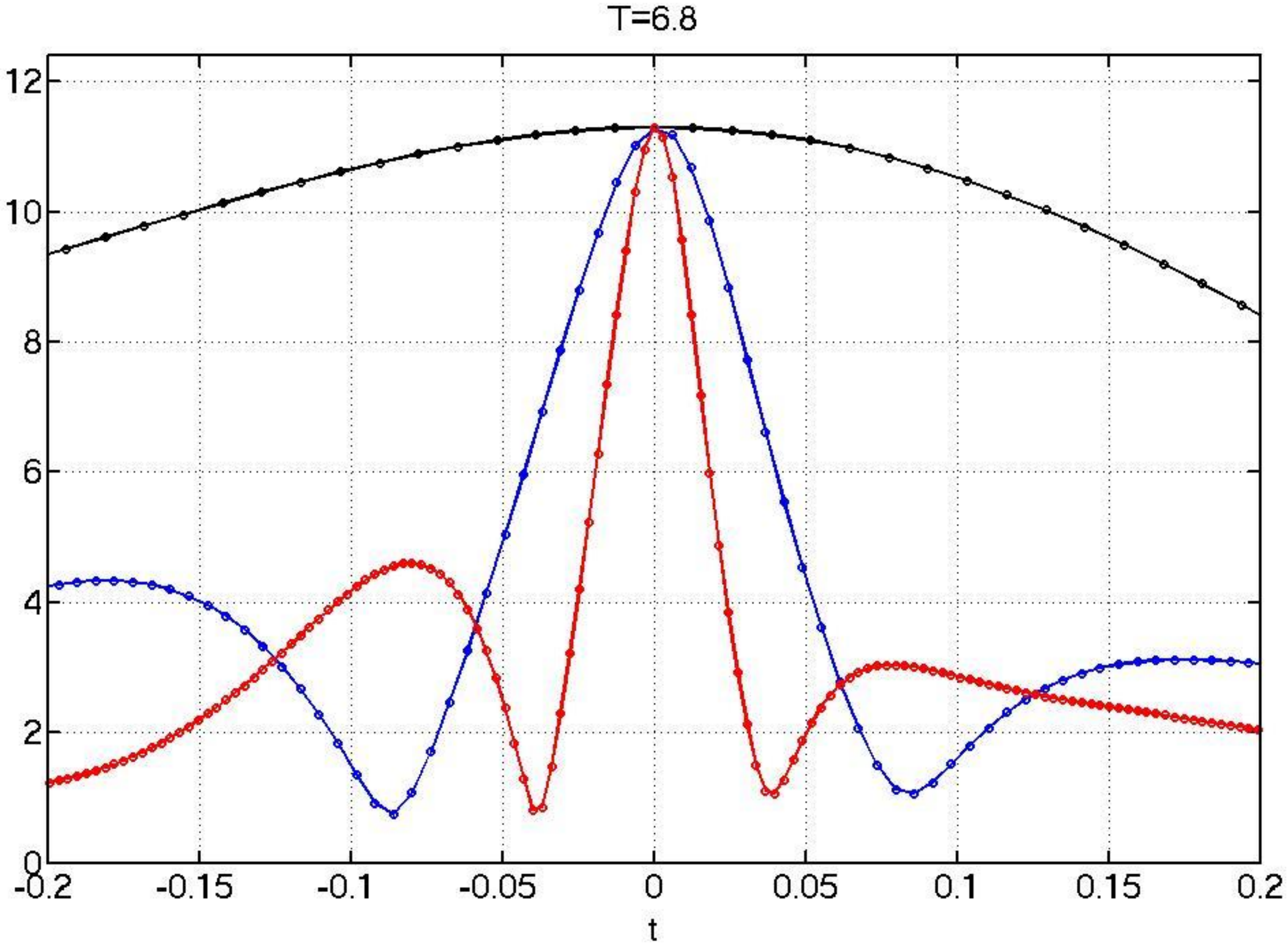

Vorticity field along the grid axis (global maximum).